Published in final edited form as:

Cell Rep. 2021 April 06; 35(1): 108930. doi:10.1016/j.celrep.2021.108930.

Insight into the human pathodegradome of the V8 protease from *Staphylococcus aureus*

Andrew Michael Frey[1], **Dale Chaput**[1], **Lindsey Neil Shaw**[1,2,*]

[1]Department of Cell Biology, Microbiology & Molecular Biology, University of South Florida, Tampa, FL 33620, USA

[2]Lead contact

SUMMARY

Staphylococcus aureus possesses ten extracellular proteases with mostly unknown targets in the human proteome. To assist with bacterial protease target discovery, we have applied and compared two N-terminomics methods to investigate cleavage of human serum proteins by *S. aureus* V8 protease, discovering 85 host-protein targets. Among these are virulence-relevant complement, iron sequestration, clotting cascade, and host protease inhibitor proteins. Protein cleavage sites have been identified, providing insight into the disruption of host protein function by V8. Complement proteins are cleaved within peptidase and sushi domains, and host protease inhibitors are cleaved outside their protease-trapping motifs. Our data highlight the potential for further application of N-terminomics in discovery of bacterial protease substrates in other host niches and provide omics-scale insight into the role of the V8 protease in *S. aureus* pathogenesis.

Graphical abstract

*Correspondence: shaw@usf.edu.

AUTHOR CONTRIBUTIONS

A.M.F. designed, performed, or assisted in all experiments and data analysis and wrote the manuscript. D.C. performed mass spectrometry, assisted with data analysis, and provided support and guidance for manuscript and sample preparation. L.N.S. initially conceived of the project, provided experimental design input, and wrote and edited the manuscript.

SUPPLEMENTAL INFORMATION

Supplemental information can be found online at https://doi.org/10.1016/j.%20celrep.2021.108930.

DECLARATION OF INTERESTS

The authors declare no competing interests.

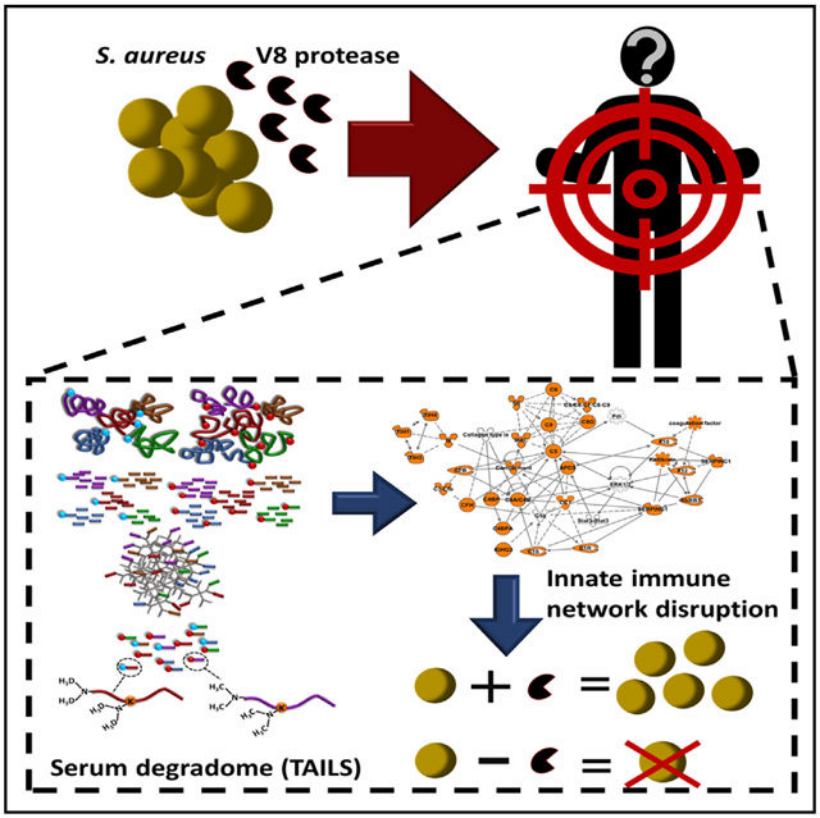

In brief

S. aureus-secreted proteases are central to disease causation, but the discovery of their host substrates has been limited. Frey et al. use N-terminomic approaches to uncover human serum targets of the V8 protease that are from virulence-relevant processes such as the host inflammatory network and nutrient sequestration.

INTRODUCTION

Staphylococcus aureus is speculated to be among the most common causes of human disease. Key to its success is an arsenal of virulence determinants, including hemolytic factors, exoenzymes, and a cadre of toxins, all of which ensure the survival of *S. aureus* during interaction with the host immune system. Produced alongside these are ten extracellular proteases: a metalloprotease (aureolysin, *aur*), a V8 (SspA) serine protease, two cysteine proteases (staphopain A [ScpA] and staphopain B [SspB]), and 6 serine-protease-like enzymes (SplABCDEF) (Reed et al., 2001; Shaw et al., 2004). Despite the first of these enzymes being identified >40 years ago (Drapeau et al., 1972), their role in virulence has remained, until recently, largely unclear. In an early study by Coulter, a V8 protease mutant was shown to be attenuated in 3 separate animal models of infection (Coulter et al., 1998). Our group demonstrated reduced virulence of *sspA* (V8) and *sspB* mutants using a murine abscess model (Shaw et al., 2004). Conversely, in this same study we demonstrated no alterations in virulence for *aur* and *scpA* mutants. Work by others has shown that a non-polar

sspA (V8) mutant has no altered virulence in wound formation (Rice et al., 2001), and we have shown that *sspA*, *sspB*, *aur*, and *scpA* mutants have no alteration in virulence using a murine model of septic arthritis (Calander et al., 2004). Both staphopains induce vascular leakage and shock in a guinea pig model of infection (Imamura et al., 2005), while an *splABCDEF* mutant demonstrated no decrease in virulence using a murine peritonitis infection model (Reed et al., 2001).

More recently, our group analyzed a *S. aureus* strain (Δprotease) with all 10 proteases deleted (Kolar et al., 2013), finding that protease ablation increases the killing of infected mice. Proteomic analysis revealed that toxin and exoenzyme abundance had increased in cultures of Δprotease (Kolar et al., 2013). Thus, in the absence of proteolytic activity, *S. aureus* virulence factors exist unchecked, providing the potential for highly aggressive infections. Accordingly, secreted proteases appear to be master regulators of virulence, by controlling the stability of *S. aureus* virulence factors.

Converse to this, Δprotease displayed impaired blood survival, decreased phagocytosis resistance, increased sensitivity to AMPs, and impaired dissemination and/or survival during infection. Thus, the impairment in virulence of Δprotease stems from a key role for these enzymes in attacking the host, cleaving proteins that facilitate nutrition, immune evasion, and movement to new sites of infection. This notion is supported by *in vitro* literature where *S. aureus*-secreted proteases have been shown to cleave numerous human proteins, including elastin, plasminogen, fibronectin, fibrinogen, the heavy chains of all human immunoglobulin (Ig) classes, high-molecular-weight kininogen, human α1-proteinase inhibitor, α1-antichymotrypsin, and complement components (Wegrzynowicz et al., 1980; Potempa et al., 1986, 1988; Proke sová et al., 1992; Imamura et al., 2005; Beaufort et al., 2008; Nickerson et al., 2010; Laarman et al., 2011; Jusko et al., 2014).

A major bottleneck to the study of proteases has been the slow and complex nature of substrate identification. Much of the work performed thus far on *S. aureus* proteases has made use of purified protein and immunoblotting strategies, leading to a one-at-a-time approach for target identification. Recent advances in proteomics has, however, made the global and rapid identification of proteolytic cleavage events possible, leading to the emergence of the proteomics sub discipline of degradomics (Marshall et al., 2017), a process that allows for the enrichment of N and C termini followed by their detection and quantification. These methods aim to detect native termini of intact proteins but also any proteolytic cleavage event that generates neo-N and C termini within the native protein sequence. Degradomics, particularly N-terminomics, has been applied to a diverse array of *ex vivo* studies of cell signaling (Overall and Dean, 2006; Kleifeld et al., 2010; auf dem Keller et al., 2013) and *in vivo* studies of conditions such as cancer (Prudova et al., 2016) and wound healing (Sabino et al., 2015). Infectious organisms have also been the subject of N-terminomic studies, highlighting transcriptional and translational regulation, as well as post-translational modification or protein activation, as seen for the opportunistic pathogen *Listeria monocytogenes* (Impens et al., 2017) and livestock pathogen *Mycoplasma hyopneumoniae* (Berry et al., 2017). Discovery of previously unknown host substrates of viral proteases from Poliovirus and Coxsackievirus (Jagdeo et al., 2018) and Zika virus (Hill et al., 2018) using N-terminomics has also been recently described. However, with the

exception of the work by Overall and colleagues during development of the TAILS N-terminomics method (described below), where fibroblast secretomes were degraded by bacterial GluC/V8 for the purposes of method validation (Kleifeld et al., 2010), N-terminomics approaches have not been used to study the impact of proteolysis at the host-bacteria-interface, or in discovery of novel host targets of bacterial proteases (Marshall et al., 2017).

Of the *S. aureus*-secreted proteases, V8 is perhaps the most well understood, being first described in the 1970s (Drapeau et al., 1972), with its high proteolytic activity but strict specificity for cleavage after glutamic acid (and to a lesser extent aspartic acid residues) being well established (Drapeau et al., 1972; Sørensen et al., 1991). Therefore, to begin our investigation of protease-host substrate interactions, we selected the V8 protease and assessed its ability to cleave human serum proteins, an infection relevant source of soluble substrates. Serum contains previously characterized V8 substrates, established by conventional low-throughput approaches, such as immunoblotting (Shohet et al., 1993; Jusko et al., 2014), allowing for internal validation of cleavage events. The ability of two N-terminomic approaches to elucidate the serum N-terminome and V8 substrates in serum was compared: aminobiotinylation (Timmer and Salvesen, 2011) and terminal amine isotopic labeling of substrates (TAILS) (Kleifeld et al., 2010). We identified ~90 host-protein targets of the V8 protease in human serum, highlighting the contribution of this protease to *S. aureus* virulence by disruption of multiple components of host complement and clotting cascades, and degradation of host protease inhibitors.

This study of the human serum N-terminome also presents the pathodegradome of a bacterial proteolytic enzyme. We suggest that the continued deployment of these approaches has the potential to facilitate our understanding of niche/organ/tissue specific infections and generate future therapeutics for the treatment of *S. aureus* diseases.

RESULTS

A comparison of N-terminomic methodologies for identification of host targets of the staphylococcal V8 protease

We began by exploring two N-terminomic methods, a positive selection technique that employs aminobiotinylation (abbreviated to Biotin in figures), and a negative selection protocol known as TAILS (Figure 1; Kleifeld et al., 2010; Timmer and Salvesen, 2011). Using the former method on pooled human serum, a total of 91 unique peptides from 34 unique proteins (Figure 2; Table S1) were identified across conditions. An explanation for this lower-than-expected number of proteins and N-terminal peptides may be the stringent parameters used during spectral assignment in MaxQuant, and subsequent exclusion of peptides present in only 1 biological repeat. That said, whole proteome approaches by others have identified ~500–~1,500 proteins in human serum (Chromy et al., 2004; Lan et al., 2018). We next sought to improve our N-terminome coverage by albumin depletion (AD), which has been shown to improve coverage of the proteome (Chromy et al., 2004; Haudenschild et al., 2014). Upon analysis, we actually observed a decrease in coverage following albumin depletion, with only 66 unique peptides identified from 44 unique proteins. Comparing the depleted and intact analyses, 48 peptides and 29 proteins were

shared across both tests, which represents 44% and 54% of total unique peptides and proteins in both conditions.

To determine whether the seemingly low number of proteins/ peptides identified using aminobiotinylation was indicative of limited V8 targets within human serum, or a lack of sensitivity of the method, we next employed TAILS. Here, we noted a substantial improvement in serum N-terminome coverage compared to aminobiotinylation, detecting 549 unique peptides from 150 unique proteins (Figure 2; Table S1) when peptides detected in serum and AD serum were combined. In contrast to aminobiotinylation, AD did increase coverage of the N-terminome, from 384 unique peptides and 122 unique proteins in serum, to 433 unique peptides from 137 unique proteins in AD serum. Combining serum and AD serum yielded a total of 549 unique peptides from 150 proteins, with 48.7% and 66.2% of total unique peptides and proteins present in both serum and AD serum.

We next sought to assess the ability of these two methods to identify V8 cleavage events within human serum proteins. The catalytic specificity of the V8 enzyme is well known, with a primary preference for cleavage at glutamic acid (glu, E) residues, and, to a lesser extent, at aspartic acid (asp, D) (Sørensen et al., 1991). Therefore, the unique peptides representing neo-N termini in V8-treated conditions should occur downstream of E or D residues in the protein sequences identified. When analyzing data across serum and AD serum with aminobiotinylation, we detected neo-N termini (peptides unique to V8-treated serum or AD serum, and significantly increased in abundance relative to untreated controls) with E or D residues (P1) in 36/61 (59%) peptides (Figure 3A). This result was some-what unexpected, given the known preference of V8 for E or D residues. It is possible that the 41% of cleavage events found at residues other than E or D result from host proteolytic processing events or N-terminal ragging (Lange et al., 2014; Marino et al., 2015). Upon analyzing data derived from our TAILS analysis, we did observe greater enzymatic specificity, with 206/280 (74%) of neo-N-terminal peptides from the V8-treated conditions possessing an N-terminal E or D residue (Figure 3A).

Using IceLogo (Colaert et al., 2009), we established residues displaying significantly increased frequency surrounding putative cleavage sites (Figures 3B and 3C). In TAILS, only E was significantly increased at P1 (i.e., directly upstream of the scissile bond), while for aminobiotinylation R was also significantly increased alongside E, to a lesser extent. Both enrichment methods highlighted a small but significant increase in G at P1′, T at P2′, and V at P4′. Cleavage sites with E/D at P1 from the TAILS dataset were aligned and compared using IceLogo in an attempt to uncover a consensus sequence or preferences for residues surrounding the E or D at P1 (Figure S1). Besides these residues at P1, almost all 20 encoded amino acids were observed at least once in residues P5-P5′ surrounding the scissile bond. The exceptions to this were an absence of W at P5 and P5′, M at P2, and P at P3 and P1′. While the absence of W and M could be coincidence due to their low abundance in eukaryotic proteomes (UniProtKB/Swiss-Prot protein knowledgebase, release 2018_09), proline was present in 4%–8% of residues in P4–P5, P1–P2, and P2′–P5′, as expected given the abundance of proline in the proteome. The absence of Pro at P3 and P1′ (but not M and W at these aforementioned positions) was identified as a significant reduction by IceLogo (Figure S1). Therefore, the presence of Pro at P3 or P1′ may inhibit the activity of V8 at a

given E/D residue or be indicative of sites where this enzyme does not cleave proteins in their native state. The inhibitory effect on V8 of proline at P1′ (and to a lesser extent P3) is also observed in the MEROPS database (https://www.ebi.ac.uk/merops, [Rawlings et al., 2018], MEROPS: S01.269, glutamyl endopeptidase I). While Pro flanking the scissile bond has a detrimental effect on protease activity in general, as determined by *in vitro* biochemical assays (Brömme et al., 1986; Markert et al., 2003), our *ex vivo* data build on this by utilizing a host substrate source for V8 that specifies an absence of Pro at P3 and P1′, providing some guidance for prediction of V8 cleavage sites in other host substrates.

Regarding methodology, combined analysis of both serum and AD serum samples during N-terminomics improves N-terminome coverage, compared to either serum or AD serum alone, and TAILS results in greater coverage of the serum N-terminome than aminobiotinylation. The identified consensus sequence for V8 cleavage also validates the N-terminomics methods, particularly for TAILS, since E was the only significantly prevalent residue at P1: 74% of P1 residues upstream of Neo-N termini in V8-treated conditions. The discrepancy between aminobiotinylation and TAILS with regards to correct identification of cleavage specificity might be explained by a small amount of NHS-SS-sulfobiotin reagent being present during (and following) tryptic digestion for aminobiotinylation, despite desalting/ cleanup prior to trypsinization. This holds some credence given that R was a prevalent residue at P1 following aminobiotinylation, but not TAILS. Regarding the increased N-terminome coverage in TAILS versus aminobiotinylation, serum proteins have been shown to bind non-specifically to streptavidin-coated surfaces, inhibiting assays for biotinylated peptides (Norton et al., 1996). It could be the case that tryptic serum peptides display similar non-specific binding to streptavidin, inhibiting enrichment of the N-terminome in this method, a drawback that TAILS does not suffer from, since the HPG-ALD polymer relies on binding to tryptic peptides.

Assessment of TAILS efficacy by comparison to pre-enriched samples

A portion (50 μg) of each sample underwent preparation and subsequent MS/MS analysis, but without exposure to HPG-ALD polymer after tryptic digest. This enabled a matched comparison of N-terminome coverage pre- and post-enrichment by HPG-ALD polymer (termed pre-TAILS and TAILS peptides). Although these had to be searched with variable N-terminal modifications, MaxQuant output files identify N-terminally dimethylated peptides in each condition, distinguishing protein (or cleaved protein) N-terminal peptides from those produced by tryptic digest. The pre-TAILS peptide lists underwent the same data processing as those in the TAILS (HPG-ALD enriched) samples, and the subsequent N-terminal peptide lists were compared. Across conditions pre- and post-enrichment, a total of 624 unique N-terminal peptides were identified, with 380 unique peptides across pre-enriched (pre-TAILS) samples, and 549 unique peptides across enriched (TAILS) samples (Figure S2; Table S2). Of the total N-terminal peptides, 12% were exclusive to pre-TAILS, 39% were exclusive to TAILS, and 49% shared between the pre- and post-enriched conditions. When N-terminal peptides unique to the V8 conditions pre- and post-enrichment are compared, these proportions remain similar (10%, 39%, and 51%, respectively). Enrichment can be considered effective given that TAILS successfully identified 89.6% of

all unique N-terminal peptides; without enrichment, 61.5% of unique N-terminal peptides were detected.

N-terminomics predicts V8 targeting of serum proteins with relevance to *S. aureus* pathogenesis

TAILS identified 280 putative V8 cleavage sites (Table S3). These occurred in 85 unique proteins (Table S4). The majority of cleaved proteins possessed immunological functions, being Igs, complement components, or multifunctional immunoregulators or were part of the clotting cascade. A number were host protease inhibitors or involved in nutrient sequestration, including iron, and thus are also relevant to *S. aureus* pathogenesis. To validate these findings, several substrates underwent immunoblotting. These included previously described V8 substrates: Complement components C3 and C4b (Jusko et al., 2014), SERPINA1 (α−1-antitrypsin) (Rapala-Kozik et al., 1999), and (pro)thrombin (Prokesová et al., 1992) and putative V8 substrates identified herein: SERPINC1 (antithrombin-III), α−2-macroglobulin, and serotransferrin. Blots were performed on serum that had been incubated in variable concentrations of V8, with the goal of qualitative cleavage assessment and observation of cleavage fragments. Linear schematics of substrates are shown adjacent to their respective blots, including V8 cleavage sites suggested by TAILS, highlighting processing in the context of the native protein and functional domains (Figure 4). For the complement proteins C3 and C4, native proteolysis as part of complement activation appears to occur, even in untreated controls, as evidenced by bands at ~70–80 kDa, which may correspond to the β chain of C3 (predicted mass 71 kDa), or the β chain or α chain of C4 (72 and 84 kDa). For C3, V8 cleavage sites occurred before residues 431, 465, 754, 978, 1178, 1405, 1517, 1531, 1532, 1567, and 1573, i.e., in both C3a and C3b. The major V8-degradation product of C3 observed in the western blot (~50 kDa) may correspond to the β chain cleavages predicted by the TAILS N-terminomics data at residues 431 and 465. For C4, TAILS identified multiple V8 cleavage sites in the α chain, at residues (P1′) 760, 960, 962, 993, 972, 1103, 1604, 1281, and a single cleavage site in the γ chain at 1604. The degradation pattern could be explained by the multiple cleavages occurring at residues 960–993, consistent with the shift in position of the major band in the C4b western blot, if this band corresponds to the C4d-B fragment of the α chain. Alternatively, the three putative cleavage sites in close proximity (at residues 960, 972, and 993) may result in degradation of the α chain into two products including one of ~50 kDa in mass, resulting in the observed degradation product in the C4 western blot.

Regarding the host protease inhibitors, α−2 macroglobulin (A2M) was also extensively cleaved by V8, including in the bait region (BR), which is typically responsible for covalent binding and inactivation of serine proteases. In our studies, the area surrounding the BR was also cleaved by V8, suggesting targeted inactivation of A2M by *S. aureus*. Four V8 cleavage sites were detected upstream of the A2M N-terminal Ig-like fold, while two were present in the C-terminal Ig-like fold. V8 cleavage at these positions may act to destabilize A2M tertiary structure and could result in an inability to trap proteases, since conformational change subsequent to cleavage of the BR is a key part of inhibitory activity (Bowen and Gettins, 1998), where A2M encloses the active site of a target protease. Furthermore, the receptor binding domain (RBD) of A2M, which functions in the clearance of activated

A2M-protease complexes, was also cleaved. The inter-α-trypsin (ITIH) and SERPIN families of protease inhibitors were also identified as V8 substrates. Immunoblotting performed against SERPINA1 and SERPINC1 confirmed their cleavage in a manner predicted by our N-terminomics data. SERPINs are characterized by the presence of an ~400 residue SERPIN domain (key to heparin-regulation of this inhibitor), and a reactive center loop (RCL) at their C terminus, which possesses a function analogous to the BR of A2M. For both SERPINA1 and C1, V8 produced three cleavage sites in close proximity, N-terminal to the RCL. For SERPINA1, cleavage occurred at P1′ residues 281, 291, and 293, ~100 residues upstream of the RCL, while for SERPINC1 cleavage occurred at 407, 411, and 414, at the N terminus of the RCL (RCL is positioned between residues 411–439 of SERPINC1). Notably, the motifs encompassing both sites are rich in E residues. In addition to evasion of the protease-trapping mechanism in a fashion similar to A2M, inactivation of SERPINs may be directly relevant to pathogenesis, with epithelial cell-derived SERPINs (SCCA1 and SCCA2) shown to inhibit *S. aureus* cysteine protease degradation of SERPINs (Kantyka et al., 2011) thereby preventing entrapment. Degradation of SERPINA1 could also act indirectly during pathogenesis by enhancing host protease-mediated tissue damage. Neutrophil elastase can cause tissue damage and is inhibited by SERPINA1, but the host-derived MMP-9 (gelatinase-B) regulates this inhibitory effect by degrading the SERPIN (Liu et al., 2000). Thus, V8 may enhance host tissue damage indirectly through dysregulation of neutrophil elastase.

In addition to immuno-relevant protease inhibitors and complement proteins, V8 cleavage of thrombin was also validated. In untreated serum, immunoblotting with anti-prtH revealed intact prothrombin, activated thrombin, and the intermediate prethrombin, while in V8-treated conditions these bands were absent, with no degradation products. This may be due to the use of a monoclonal antibody, specific to a region at residue ~322 (proprietary information not disclosed by the manufacturer), in close proximity to the N-terminomics-inferred V8 cleavage sites between residues 298–299 and 371–372. Notably, N-terminomics highlights that V8 cleaves close to the N terminus of the heavy thrombin chain—*in vivo* this cleavage event may act in synergy with native proteolytic activation of thrombin.

Finally, the key host iron sequestration protein serotransferrin was indicated to be extensively cleaved by V8 and was subsequently chosen for immunoblotting. The intact protein can be observed in the western blot, alongside degradation products in the V8-containing conditions. These degradation products at ~49, 40, and ~25 kDa correspond closely to those predicted by N-terminomics. Notably, both transferrin domains appear to be cleaved by V8, which may result in iron release *in vivo*, contributing to *S. aureus* survival and pathogenesis.

In addition to confirmation of proteolysis via western blotting, specific cleavage events in A2M and C3 were also assessed using recombinant protein to validate cleavage sites identified by TAILS. Purified C3 and A2M were subjected to V8 digestion, followed by SDS-PAGE and in-gel tryptic digest of degradation products (Figure S3A). For both proteins, bands corresponding to the approximate size of degradation products in the western blot were selected, along with some lower-mass bands. Following MS/MS and spectral assignment in MaxQuant, the resulting V8-specific, semi-tryptic peptides (i.e., those with

Glu or Asp residues proceeding the peptide N terminus, or Glu or Asp at the peptide C terminus) were used to validate TAILS-identified cleavage sites (Table S5; Figure S3). For both proteins, substantially more peptides with V8-semi-tryptic specificity were observed than were detected following TAILS. The majority of TAILS-identified V8 cleavage sites were covered in this approach, with 7/10 observed for C3, and 3/8 observed for A2M. In the latter protein four TAILS-identified cleavage sites are in close proximity, perhaps accounting for the discrepancy (Figure S3B). The absence of other TAILS-identified cleavage sites may be due to the size exclusion innate to selecting degradation products (protein bands) following SDS-PAGE, and perhaps other degradation products are of low mass and thus completely lost due to high electrophoretic mobility.

N-terminomics highlights V8 cleavage of multiple components of inflammatory signaling pathways

An unbiased analysis of host protein network disruption by V8 was performed using the interaction analysis feature of IPA software (QIAGEN). Usually used to describe possible impacts of expression changes, here proteins cleaved by V8 were assigned as significantly dysregulated (up- or down-regulated) with 95% certainty, to reflect the t test p value of 0.05 used to determine significant changes in peptide intensity between untreated and V8-treated conditions. An acute phase response/innate inflammatory network was significantly influenced, containing a number of V8 substrates (Figure 5; Table S4). Three functional clusters can be observed: the complement and clotting cascades, and protease (inter-α-trypsin) inhibitors. While the latter group of inhibitors do not form a distinct inflammatory cascade themselves, they prevent excessive propagation of the complement cascade (Salier et al., 1996) and indirectly impact the clotting and complement cascades by limiting degradation of vitronectin.

In addition to identifying previously described V8 cleavage of clotting proteins prothrombin (Suzuki et al., 1990) and kininogen (Molla et al., 1989), the serine protease inhibitors SERPING1, SERPINF2, and SERPINC1 were V8 substrates highlighted in the clotting cluster, with all three known to inhibit factor XII, the latter also inhibiting factor X activity. Interestingly, factor X and factor XII were also identified as V8 substrates in our experiments, though each only possessed a single putative V8 cleavage, with Neo-N termini produced at residues 418 and 452 in the activated forms of the two factors. These cleavage events fall within the heavy chain of factor X and light chain of factor XII, domains that contain the serine protease responsible for propagation of the clotting cascade when the factors are activated. The impacts of V8-mediated proteolysis on coagulation in the context of infection are difficult to interpret given that induction of coagulation is a hallmark of *S. aureus* colonization (Loeb, 1903), through the secretion of *S. aureus* coagulase (Coa), von Willebrand binding factor (vWbp), and the fibrinogen binding clumping factors (ClfA-B), which enhance coagulation (McAdow et al., 2012). That said, prevention of clot formation could contribute to dissemination, and V8 may function in this capacity. This notion of proteases assisting dissemination by cleavage of host factors fits with the phenotypic switching seen during *S. aureus* growth, where a population of *S. aureus* reaches a sufficient density, inducing the Agr quorum sensing system, which promotes protease production and reduces biofilm formation (Boles and Horswill, 2008). Although the mechanism for this

appears to be protease-mediated degradation of *S. aureus* adhesins (Kolar et al., 2013; Byrum et al., 2018), secreted protease activity may also degrade host factors, contributing to detachment and biofilm dispersal.

Components of the complement cascade, including ficolin-3, C1s, C1r, C3, C4, C4BPA- (complement 4 binding protein α chain), C5, C6, C8G, C9, CfB, and CfH, were all identified as V8 substrates. Some of these (C3, C4, ficolin-3, CfB, C5) have been previously highlighted as V8 substrates (Jusko et al., 2014), though, given their multi-functional nature, with different complement protein fragments possessing their own distinct functions during activation of the intact protein, the location of cleavage sites within complement proteins is of particular importance. The precise complement-V8 cleavage sites identified here could be assigned to domains with described functions, which were binding or association with other complement components or immune cells, proteolytic activation of other complement components, or formation of the membrane attack complex (MAC) in the late stages of complement activation. CUB and Sushi domains (ExPASY prosite annotation rules PRU00059 and PRU00302, a wide variety of domains involved in numerous recognition processes) were prominently cleaved by V8 (Table S3). C1r proteolytically activates C1s, which in turn proteolytically activates C2 and C4. Here, V8 was shown to cleave both C1r and C1s within CUB domains of both components (N-terminal to residue 44 in C1r, and 208 in C1s), which are key to close association and interaction between the two (Almitairi et al., 2018). The proteolytic activity and subsequent activation of C2/C4 by C1s is also likely to be abrogated by V8, since the S1 peptidase domain of C1s was cleaved (N-terminal to residue 355). C3 and C4b were extensively cleaved by V8, with a total of 12 and 11 neo-N termini found throughout C3 and C4 after V8 treatment. C3b (residues 749–1663) was extensively cleaved (with neo-N termini at 754, 978, 955, 1178, 1405, 1532, 1567, 1531, 1517) as was C4b. In their intact, native state C3b and C4b form C3 convertases with C2, which activate C5. The ability of V8 to degrade the C3b chain may synergize with the activity of Aur, which cleaves intact C3 into active C3a and C3b distal to the bacterial cell surface (i.e., the intended target of C3), and, while host factors were previously shown to degrade Aur-generated C3b (Laarman et al., 2011), N-terminomic data shown here indicate that V8 bolsters C3b degradation, which would downregulate the late complement cascade, the next component of which is C5. C5 was cleaved within its alpha chain (residue 938), which is involved in formation of the MAC. Regarding other MAC components, C6 was cleaved N-terminal to residue 266, within its MAC/perforin domain (MACPF), and also at residue 712, within a Sushi domain; thus, V8 may disrupt C6 interactions with other complement components, and the target cell membrane. C8 was cleaved by V8 within the C8γ domain, a lipocalin that forms a β-barrel in target cell membranes and was recently shown to function in part by complexing with C8α (a MACPF domain) (Slade et al., 2008). The final protein of the MAC, C9, was cleaved by V8 close to the middle of the protein sequence (residue 258), within the MACPF domain. Outside of the complement components 1–9, complement factors B and H were also targets of V8. CfB is cleaved into two components, CfBa and CfBb. CfBb is the proteolytic component and acts during alternative complement activation to generate C3 and C5 convertases. V8 appeared to cleave twice at its active site, where CfbB residue 699 is involved in charge relay during catalysis (as annotated in UniProt); TAILS showed cleavage N-terminal to residues 699 and 685. In contrast to the

general observation that V8 inhibits propagation of the complement cascade, we also observed degradation of CfH, an inhibitory complement factor, which primarily limits complement activation by degradation of C3 convertases. However, binding of CfH to pathogens may act to enhance the innate immune response, as observed in *Candida albicans*, where CfH has been shown to bind neutrophils and *C. albicans*, enhancing clearance of the fungus (Losse et al., 2010). CfH was cleaved within three of its Sushi domains, N-terminal to residues 45, 722, 771, and 786.

Finally, the interaction analysis network included proteins not observed in the N-terminome (most of which were intracellular and thus not expected to be found in serum). Several of the identified V8 substrates are known to act (through intermediates) with the ubiquitously expressed extracellular signal related kinases 1 and 2 (ERK1/2, ERK not observed in the N-terminome), which were also highlighted during our analysis. ERKs are intracellular phosphokinases, activated by a variety of plasma membrane receptors in response to pro-inflammatory stimuli (Roux and Blenis, 2004). ERK signaling is directly relevant to *S. aureus*-host immune cell interactions and is susceptible to perturbation by secreted proteases, as seen for ScpA, which degrades the neutrophil CXC chemokine receptor 2, resulting in decreased ERK-mediated neutrophil migration (Laarman et al., 2012). Thus, it is possible that V8 may act synergistically with ScpA to facilitate a general downregulation of ERK-mediated pro-inflammatory signaling. The inhibition of ERK signaling by proteases contrasts with its observed upregulation following *S. aureus* attachment and invasion of host cells (Ellington et al., 2001). However, protease expression is greatest in the later phases of *S. aureus* growth (Shaw et al., 2004); therefore, *S. aureus* may exert a bi-directional impact on host ERK signaling, upregulating it via adhesin-mediated attachment and invasion during the early stages of infection, but later downregulating it through the action of secreted proteases, including V8.

Structural features of the V8 protease seemingly limit the genetic manipulation of its encoding gene

We next set out to ascertain whether natively produced V8 from *S. aureus* cells recapitulated the above findings. Such an approach would benefit from allowing serum-proteolysis experiments using the native enzyme in the presence of the entire *S. aureus* secretome, and to assess the impact of V8 on *S. aureus* survival. Producing a V8-complement proved problematic, however, but not entirely unsuccessful. First, each of our attempts to clone the gene encoding V8 (*sspA*) under the control of its own promoter either failed to produce clones in *E. coli* or were revealed to be mutated upon sequencing. This is noteworthy because an extensive literature search revealed that despite V8 being under investigation since the 1970s and a number of *sspA*-deficient strains being generated (Rice et al., 2001; Shaw et al., 2004; Nickerson et al., 2008; Loughran et al., 2014), a strictly native V8-complemented strain with its own (or any) promoter does not appear to have been produced. We suggest the reason for the inability to clone *sspA* lies in the C terminus of the V8 enzyme, described in UniProt (accession number P0C1U8) as a region containing 11 3 3 amino acid repeats of P-[DN]-N at positions 289–324. This region is predicted to be disordered (http://prdos.hgc.jp/cgi-bin/top.cgi), and a BLAST search of the C-terminal amino acid sequence (excluding results from *S. aureus*) revealed the closest homologs to be

membrane proteins in both Gram-positive and -negative bacteria (the top two hits were a BspA family leucine-rich repeat protein from *Lachnospiraceae*, and an autotransporter Beta-barrel domain containing protein from *Brucella*). Thus, we hypothesized that even low-level expression of *sspA* from its native, SigmaA promoter (Shaw et al., 2004) could be detrimental to the viability our *E. coli* cloning strain. Mechanistically, such toxicity could be explained by the N-terminal secretion signal of V8 permitting sec-dependent export across the inner membrane, at which point the C-terminal region results in V8 embedding in the inner or outer membrane, localized to the periplasm. In support of this notion, we did successfully generate a pMK4 (Sullivan et al., 1984) shuttle vector construct containing a truncated version of *sspA* under the control of the native promoter, in which the C-terminal region (from residue 285) was excluded during initial PCR from USA300 LAC genomic DNA (OL5521 and OL6018, pMK4-*sspA*$^{\blacklozenge CTD}$). We also note that the crystal structures for V8 lack the C-terminal region (Protein Data Bank accession numbers 2O8L, 1QY6, and 1WCZ), with authors speculating that loss of the C terminus during expression in *S. aureus* is due to autocatalytic activity (Prasad et al., 2004).

We note that an example of *S. aureus* complemented with tagged V8 (C-terminal 6-histidine) does exist but was utilized in biochemical studies as opposed to virulence models (Nickerson et al., 2007). This not-strictly native V8 complement was the only published example of V8 complementation we could find, besides our study here. Presumably the C-terminal 6-His tag is what permitted cloning using the *E. coli* intermediate strain in the aforementioned study. We did consider creating a plasmid encoding the C-terminally tagged V8 protease, but as indicated by crystal structures (described above) the C-terminal tail is absent in the native, mature secreted protein, while tagging results in the C-terminal tail being retained, so this option was ruled out. Complementation using our C-terminally truncated V8 (pMK4-*sspA*$^{\blacklozenge CTD}$) plasmid was an option, but we were unsure what impact this artificial C-terminal deletion might have on V8 expression, activation, and *S. aureus* viability. Instead, we were able to generate a plasmid encoding native *sspA* under the control of a cadmium inducible promoter.

Further validation of degradomics findings are confounded by the requirement for aureolysin in V8 activation

The experimental design articulated above presents a problem, as native V8 is secreted as a zymogen (Drapeau, 1978; Shaw et al., 2004), inactive without aureolysin (Aur, encoded by *aur*)- mediated proteolysis. Attempts were made to delete the zymogen-encoding region (while retaining the secretion signal), without success. This necessitated that our experiments take place using an Aur replete strain, or with co-cultures of *aur* or *sspA*-complemented into Δprotease. Therefore, *aur* was also cloned into the cadmium inducible vector, transduced into the Δprotease strain and V8-deficient (Δ*sspA*) strains, and empty vector (EV) strains were also created (Table S6).

Zymography (Figure 6A) indicated restoration of V8 and Aur activity in the Δprotease strains when complemented with *sspA* and *aur*. In the case of V8, proteolysis was only observed in the Δprotease +*aur*/*sspA* co-culture, indicating that this co-culture approach does follow the Aur-SspA activation cascade observed by others (Drapeau, 1978; Shaw et

al., 2004; Nickerson et al., 2007). Unfortunately, this renders Aur a confounding variable in experiments investigating proteolysis by *S. aureus* culture supernatants, which were performed by immunoblot. In addition, secreted staphylococcal Ig binding protein A (Spa) bound antibodies used in all blots, obscuring resolution of human proteins and their degradation products (Figure S4, band at ~50 kDa). Therefore, *spa*-deficient strains (Table S6) were generated by transduction from the appropriate mutant in the Nebraska Transposon Mutant Library (NTML) into both the Δprotease mutant and its parent strain USA300 LAC, which were then separately transduced with *aur* and *sspA* complementing plasmids or empty vectors. This resulted in loss of the band corresponding to Spa in immunoblots (Figure S4) and made resolution of some host proteins and degradation products possible (PrtH and A2M). PrtH was only visible in secretome experiments in the *spa* mutant and was fully degraded in only the parent strain (LAC EV) and the Δprotease +*aur*/*sspA* conditions. A2M was notably degraded only in the Δprotease +*aur*/*sspA* condition in the Δ*spa* experiment, but in the *spa* replete experiment the band corresponding to A2M at ~250 kDa is degraded in the parent strain (LAC EV), Δprotease +*aur*, and Δprotease +*aur*/*sspA*.

Given the presence of Aur as a confounding variable, we set out to specifically inhibit Aur using metal sequestering reagents (Figure S5). Aur was partially inhibited by 100 mM sodium citrate, but 20 mM 1,10-phenanthroline resulted in complete inhibition of Aur proteolysis, while native V8 retained activity. As expected, V8 activity was only observed in co-cultures of Δprotease *aur*/*sspA* (as well as in the parent LAC strain). However, the presence of whole bacterial secretomes in culture supernatants appeared to be detrimental to most of our immunoblots (only A2M and PrtH were consistently detected after blots were developed), and the presence or absence of 1,10-phenathroline, and the ratio and concentration of supernatant: serum used during digestion also affected protein detection. Figure S6A shows SERPINA1 as an example of this, where 500 μg of serum protein was digested with either 1 or 0.1 mg of culture supernatant (total reaction volume 500 μl), in the presence or absence of 1,10-phenanthroline. In both cases, SERPINA1 was detected in the absence of 1,10-phenanthroline, and a small amount of degradation was visible in the LAC EV and Δprotease + *aur*, and Δprotease +*aur*/*sspA* conditions with 1 mg culture supernatant but not in the 0.1 mg condition. The presence of 1,10-phenanthroline appeared to completely prevent detection of SERPINA1 in reactions containing 1 mg of culture supernatant. We did observe that addition of 1,10-phenanthroline to reactions containing culture supernatants resulted in precipitation, likely explaining the detrimental impact of phenanthroline on protein detection, particularly where higher concentrations of culture supernatant are used. Precipitation is also likely to be detrimental to the aspects of immunoblotting methodology that rely on electrophoresis (i.e., SDS-PAGE and subsequent membrane transfer). These issues are also highlighted in Figure S6B (1,000 μg culture supernatant, 500 μg serum, reaction volume 200 μl, i.e., the reaction is 2.5-fold more concentrated than above), where A2M and SERPINA1 appeared to be depleted in conditions containing both bacterial supernatant and 1,10-phenanthroline, but both proteins were readily detected in the undigested control and purified V8-treated condition, which contain no bacterial supernatant (the purified V8-treated conditions also contained visible degradation products).

Besides the impact of phenanthroline, we speculate that the variation in blotting success is due to the numerous potential interactions of *S. aureus*-secreted proteins (both protease and

non-protease) with self- (Rice et al., 2001; Shaw et al., 2004; Kolar et al., 2013; Zheng et al., 2014) and human serum (Moks et al., 1986; Imamura et al., 2005; Smith et al., 2011; Jusko et al., 2014; Elmwall et al., 2017; Skjeflo et al., 2018) proteins. This is reflected in the successful blots for A2M and PrtH (Figure S4), where for A2M there is a high-molecular-weight band (>250 kDa) in conditions only where Aur is absent. The proteolysis of PrtH in the presence of supernatants is evident across all conditions, even the Δprotease strain. This is presumably due to activation of the clotting cascade, either as a direct response to *S. aureus*- secreted proteins, or indirectly via complement activation. The activation of the clotting cascade also infers the presence of active, confounding host proteases, which can proteolyze other serum components besides those involved in coagulation (Yang et al., 2016; Weidmann et al., 2017; Bhagwat et al., 2020) and is particularly pertinent given that numerous protease inhibitors were shown here to be degraded by V8 (discussed throughout the results and discussion section), and immunoblotting indicated that secreted *S. aureus* proteins can also bind at least one protease inhibitor (A2M, Figure S4). The interactome is made all the more complex by the effect of *S. aureus*-secreted proteases on its own secretome (Kolar et al., 2013; Zheng et al., 2014; Byrum et al., 2018), with work described here utilizing protease mutants and complemented strains with host interactions that are not fully characterized.

Native V8 impacts *S. aureus* survival in human serum

Given that the Δprotease mutant is already known to display reduced growth in serum (Kolar et al., 2013), and our N-terminomic data show a clear role for V8 in serum proteolysis, our final approach was to determine the contribution of this protease to the survival of *S. aureus* in human serum. Consequently, Δ*sspA* and the complemented strain (Δ*sspA*+*sspA*) were used in a serum infection model. The requirement for Aur in V8 activation rendered Δ*sspA* the only practical choice, as opposed to using Δprotease. We observed significant deficiencies in survival of the Δ*sspA* mutant strain at multiple time points during the 24 h assessment period. Importantly, survival was restored in the Δ*sspA*+*sspA* strain (Figure 6B and 0 h normalized 24 h growth of LAC, Δ*sspA* and Δ*sspA*+*sspA* was 139%, 92%, and 124%, respectively). Therefore, despite still possessing 9/10 of its secreted proteases, the loss of V8 is detrimental to the survival and proliferation of *S. aureus* in human serum, and arguably throughout any systemic infection.

DISCUSSION

Degradomic approaches are being increasingly applied to investigate the functional proteome, where a variety of methods have been used to describe changes besides abundance of a given protein. N-terminomics has been used to discover alternative translation initiation sites in *Listeria monocytogenes* (Impens et al., 2017) and to assess self-proteolysis in *Mycoplasma hypopneumoniae* (Berry et al., 2017) and in the apicomplexan parasite *Toxoplasma gondii* (Coffey et al., 2018). Regarding pathogen protease-host interactions, TAILS has been used in recent studies of viral proteases to discover their host substrates (Hill et al., 2018; Jagdeo et al., 2018). Here, we present a study of a bacterial protease on the infection-relevant host substrate, human serum. Despite its complexity as a substrate source, aminobiotinylation and TAILS were capable of identifying a number of

serum proteins degraded by V8 protease, showcasing the value of these methods for investigation of host pathogen interactions during *ex vivo* studies. TAILS proved particularly useful, highlighting 85 host targets of the V8 protease. The substrates identified in our study could be considered validated, since we identified previously described substrates of V8 protease, such as Ig and complement components. The majority of Neo-N termini in V8-treated conditions were located downstream of glutamic acid, matching the known preference of this enzyme, with E being the only residue significantly increased in abundance at P1 in the TAILS dataset. Moreover, from the perspective of functional validation, we observed that loss of *sspA* (encoding V8) was detrimental to *S. aureus* survival and proliferation in human serum, a phenotype restored by complementation. This comparative N-terminomic dataset for human serum also suggests that using AD and whole serum in N-terminomics experiments maximizes serum N-terminome coverage, though AD serum achieves greater coverage during TAILS, a finding in line with that described for conventional shotgun proteomics.

Arguably, the use of V8 in serum presents something of an issue due to its broad activity, and thus establishing which V8-mediated proteolytic events are most relevant *in vivo* is more difficult than for a less complex substrate source or more specific enzyme. The Spl enzymes from *S. aureus*, for example, have more specific cleavage preference (Zdzalik et al., 2013; Pustelny et al., 2014; Stach et al., 2018), and thus fewer substrates. Despite this information, Spl host substrates remain largely uncharacterized, though they have recently been shown to influence the TH1/TH17-TH2 axis and elicit IgG_4/IgE antibodies during airway inflammation (Stentzel et al., 2017). Given the proof of concept shown here for V8 protease, N-terminomics offers the prospect of discovering cryptic substrates for the Spls, and indeed any other bacterial protease, in a variety of potential host niches.

Perhaps the most striking feature of our datasets was the cleavage of host protease inhibitors by V8. The SERPINs (SERPINs A1, A3, A6, A7, C1, F2, and G1), inter-trypsin-α inhibitors (ITIH1–4), and other protease inhibitors, such as α2-macroglobulin, were identified as V8 substrates and have multiple roles during inflammation. V8 cleaved outside of the RCL/BR domains of these inhibitors, the region responsible for baiting and irreversibly binding proteases. Regarding the clotting cascade, although we highlight the potential V8-induced disruption of SERPIN-mediated inhibition of factor X and XII, and thrombin, V8 is likely to inhibit the clotting cascade given that it also cleaves these proteases.

Finally, we were able to uncover the precise cleavage sites in these key innate immune molecules. For instance, V8 disrupts complement by cleaving in a variety of domains with functions in protein-ligand association, peptidase active site domains, and in domains key to protein-protein interaction and formation of the MAC. Thus, in addition to providing a high throughput method for protease target identification, N-terminomics provides a means to establish precise mechanisms of pathogen subversion of host systems.

STAR★METHODS

RESOURCE AVAILABILITY

Lead contact—Further information and requests for resources and reagents can be made to the Lead Contact, Lindsey Shaw, shaw@usf.edu.

Materials availability—Requests for plasmids and strains described in this study can be made to the Lead Contact, Lindsey Shaw, shaw@usf.edu.

Data and code availability—The accession number for the N-terminomics mass spectrometry proteomics data and peptide identification files (the direct output from MaxQuant) have been deposited to the ProteomeXchange Consortium via the PRIDE (Perez-Riverol et al., 2019) partner repository,ProteomeXchange: PXD014797.

EXPERIMENTAL MODEL AND SUBJECT DETAILS

Bacterial strains, plasmids, and cloning—*E. coli* DH5α (Salisbury et al., 1972) was routinely cultured in lysogeny broth (LB) and LB agar, with plasmid-selective antibiotics where appropriate (ampicillin, 100 μg/ml). All *S. aureus* strains, with the exception of the RN4220 intermediate cloning strain (Kreiswirth et al., 1983) were derived from USA300 LAC, a hypervirulent community acquired MRSA strain (Pan et al., 2004), and are outlined in Table S6. All *S. aureus* strains were cultured on tryptic soy broth and agar (TSB and TSA). Where appropriate (as indicated in Table S6), to ensure selection of transposon mutants and maintenance of plasmids, the following antibiotics were included in broth and agar cultures: Chloramphenicol (10 μg/ml, Chl), tetracycline (5 μg/ml, Tet), erythromycin (5 μg/ml, Ery). Lincomycin was also included in Ery agar at 25 μg/ml. Mutants deficient in either *sspA* (encoding V8 protease) or all ten secreted proteases (Δ*sspA* and Δprotease, respectively) have been previously described (Kolar et al., 2013; Ramirez et al., 2020). Strains deficient in the *spa* gene were produced as part of this study, using the Nebraska Transposon Mutant Library (NTML) and the NTML standard protocol to switch the erythromycin (ery) resistance cassette to tetracycline (tet) resistance (Fey et al., 2013). This was then transduced using φ11 into the USA300 LAC strain (to produce Δ*spa*) as well as the protease null strain to produce Δ*spa*Δprotease. Loss of Spa was confirmed by non-specific immunoblotting (Figure S4) and also PCR using primers flanking the *spa* gene (OL5259 / OL5264). All oligonucleotides used are described in Table S6, and all plasmid insertions achieved by PCR of inserts (described below), restriction digest using NEB restriction enzymes (Table S6), and ligation using a T4 ligase kit (Promega). To create complementation constructs for *aur* and *sspA*, we first generated a new inducible promoter complementation vector based on the previously published pJB67 plasmid (Windham et al., 2016). The modification created herein switched the selective marker in *S. aureus* from erythromycin to chloramphenicol, to facilitate compatibility with other mutation markers used in our strains. This was achieved by inverse PCR of pJB67 using primers that flank the erythromycin marker (OL5681 / OL5682), enabling its deletion. This cassette was then replaced with the chloramphenicol (chl) resistance gene amplified from the pMK4 plasmid (Sullivan et al., 1984) using primers OL5649 and OL5650, creating pAFLS1. Next, the coding sequence for *sspA* and *aur* were amplified using primer pairs OL5529 / OL5530 and

OL5673 / OL5674, respectively. These were cloned into pAFLS1, producing pAFLS1-*sspA*, and pAFLS1-*aur*. Clones were confirmed by Sanger sequencing (Genewiz) using plasmid specific primers (OL4093 and OL4094). Following native sequence confirmation of their respective genes, plasmids were transformed into electrocompetent RN4220 under Chl selection, before being transduced by φ11 bacteriophage into several strains for complementation experiments (Table S6).

METHOD DETAILS

Human serum, albumin depletion, and V8 protease treatment—Human serum (type AB, pooled, catalog no. ICN2930949) was purchased from Fisher Scientific. *S. aureus* V8 protease was purchased from Sigma Aldrich (catalog no. P2922). Albumin depletion was performed using a commercially available kit supplied by Fisher Scientific (catalog no. PI85160). Prior to N-terminomics and immunoblotting, all serum or albumin depleted (AD) serum was incubated at 37°C in the presence or absence of V8 protease (5–50 μg/ml for immunoblotting, 5 μg/ml for N-terminomics) for 16 hours.Serum and AD serum concentrations were assessed using the Pierce 660 nm protein assay (ThermoFisher Scientific), and concentrations standardized (see below) prior to experimentation.

N-terminomics-aminobiotinylation—Aminobiotinylation was performed according to a method established by Timmer and Salvesen (2011), as follows: 200 μl of serum or AD serum was incubated in the presence or absence of 200 ng V8. This equates to ~2 mg of protein for AD serum, and ~10 mg of protein for serum experiments, both of which fall within the recommended starting protein mass for this methodology (1–10 mg, Timmer and Salvesen, 2011). Standardizing protein concentrations between serum and AD serum was considered, but due to the potential impact on low abundance targets in the serum conditions this was not performed. Dry guanidium hydrochloride (6 M final concentration) was added to inactivate proteases following incubation. Samples were reduced with 10 mM dithiothreitol and incubation for 10 minutes at 95°C, before being cooled to room temperature, and alkylated with 30 mM iodoacetamide for 30 minutes in the dark at room temperature (22°C). Guanidination of lysine was performed by treatment with dry O-methylisourea hemisulfate (0.5 M final concentration) at pH 11 (adjusted with NaOH) for 16 hours at 4°C. Samples were desalted using PD-10 columns (GE Healthcare) and urea buffer (8 M urea, 50 mM HEPES pH 7.8, 100 mM NaCl). N-terminal amines were biotinylated by incubation with 5 mM NHS-SS-sulfobiotin (Fisher Scientific) for 1 hour at 37°C, and the reaction quenched with 50 mM ammonium bicarbonate, pH 7.8. Removal of low-frequency ser/thr -biotin reactions was performed with 40 mM hydroxylamine hydrochloride. Samples were desalted with PD-10 columns as above and diluted with 50 mM ammonium bicarbonate to 2 M urea. Samples were digested with 4 μg sequencing grade trypsin (Promega) for 18 hours at 37°C (ratio of trypsin: protein for AD serum and serum was 1:500 and 1:2500).

Biotinylated N-termini were enriched by incubation with 500 μl of high capacity neutravidin resin (fisher scientific, equilibrated with urea buffer + 40mM ammonium bicarbonate) for 30 minutes at 4°C, with rocking. Samples were loaded onto 2 mL disposable polystyrene columns, washed with 10 column volumes of urea buffer, and three column volumes of 50

mM ammonium bicarbonate (pH 7.8), transferred to microfuge tubes, and the disulfide link between biotinylated protein and streptavidin beads reduced using 5 mM TCEP-HCl. Peptides were collected by loading samples onto micro-bio chromatography columns (BioRad) followed by centrifugation at 500 g for 30 s. Resin was washed twice with 50 mM ammonium bicarbonate, and an additional centrifugation at 10000 g was performed, with flow-through containing N-terminal peptides collected. Peptides were desalted using commercially available Sep-Pak C18 desalt columns (Waters), according to the manufacturer's instructions.

N-terminomics, TAILS—TAILS was performed according to a method established by Overall and colleagues (Kleifeld et al., 2010, 2011), as follows: Serum or AD serum was incubated in the presence or absence of V8 (see above), and standardized to 600 μg/ml. Protein must be standardized in this approach due to the use of HPG-ALD polymer (see below). Samples were incubated with 10 mM DTT for 60 minutes at 37°C, pH adjusted to 6, and alkylated with 30 mM iodoacetamide for 30 minutes in the dark at room temperature (22°C). Reactions were quenched by adding 20 mM DTT, and samples were concentrated by chloroform-methanol precipitation. Protein pellets were resuspended in 100 mM NaOH, 50 mM HEPES pH 8, and guanidium hydrochloride added to 4 M. N-terminal dimethylation was performed using either light formaldehyde and sodium cyanoborohydride (light demethylation, used for untreated conditions), or ^{13}C1 formaldehyde and sodium cyanoborodeuteride (heavy dimethylation, used for V8 treated conditions), enabling diplexing during mass spectrometry. Samples were incubated with 40 mM formaldehyde and 20 mM sodium cyanoboro- reagents for 16 hours at 37°C. A second incubation was performed with fresh dimethylation reagents added again, for 2 hours. Reactions were quenched by addition of 100 mM Tris HCl, pH 6.8, and incubation at 37°C for 1 hour. Heavy and light dimethylated samples were then combined, and 5 μg sequencing grade trypsin (Promega) was added (1: 200 trypsin: protein ratio) and incubated at 37°C for 16 hours. Hyperbranched polyglycerol aldehyde (HPG-ALD) was purchased from flintbox (https://ubc.flintbox.com/#technologies/888fc51c-36c0-40dc-a5c9-0f176ba68293), and prepared for use according to the manufacturer's protocol with 10 kDa cutoff centrifugal filters. Trypsin-digested peptides were added to HPG-ALD polymer at a polymer:peptide mass ratio of 5:1, in the presence of sodium cyanoborohydride, and incubated for 16 hours at 37°C. Fresh 10 kDa centrifugal filters were equilibrated by washing once with 100 mM NaOH and three times with HPLC grade water. Samples were loaded onto centrifugal filters with 100 mM Tris, and centrifuged for 10 minutes at 12000 g, with the flowthrough containing N-terminal peptides retained. Filters were rinsed with HPLC grade water to remove polymer, with filters placed upside down in collection tubes and centrifuged at 12000 g for 1 minute to improve recovery of hydrophobic peptides. Peptides were desalted using commercially available Sep-Pak C18 desalt columns (Waters), according to the manufacturer's instructions.

Mass Spectrometry—Following either aminobiotinylation or TAILS, and desalting, N-terminal enriched peptides were resuspended in 0.1 % formic acid, with 5 μl aliquots separated on a 50cm Acclaim PepMap 100 C18 reversed-phase high-pressure liquid chromatography (HPLC) column (Thermo Fisher Scientific) using an Ultimate3000 UHPLC

(Thermo Fisher Scientific) with a 180 min gradient (2 to 32 % acetonitrile with 0.1 % formic acid). Peptides were analyzed on a hybrid Quadrupole-Orbitrap instrument (Q Exactive Plus; Thermo Fisher Scientific) using data-dependent acquisition in which the top 10 most abundant ions were selected for MS/MS analysis.

Data Processing—MaxQuant (Cox and Mann, 2008) (https://www.maxquant.org/) was used to process raw files, assigning MS/MS spectra to the human proteome (UniProt ID UP000005640) with the included Andromeda search engine. For aminobiotinylation experiments, cysteine carbamidomethylation was set as a fixed modification (57.021464), and methionine oxidation (15.994915), lysine guanidination (42.021798) and the N-terminal biotin linker stub (reduced EZ-Link Sulfo-NHS-SS-Biotin, 87.998285) set as variable modifications. For TAILS, cysteine carbamidomethylation and peptide N-terminal and lysine dimethylation were set as fixed modifications (heavy or light modifications were assigned in separate searches), while methionine oxidation was set as a variable modification. An additional pair of searches were performed where dimethylation of N-termini was substituted for N-terminal peptide acetylation or N-terminal glutamine or glutamic acid converted to pyroglutamate (cyclization). In both methods, peptide tolerance and MS/MS tolerance were set at 5 ppm and 0.5 Da, respectively, and the scoring scheme used was ESI-TRAP. Spectra were not matched between repeats. The resulting peptide and modification specific peptide .txt files were processed further using Perseus, as follows: Files were opened as separate matrices in Perseus, and peptides present in at least two of three separate experiments (biological repeats) in any one condition (untreated serum, V8 treated serum, untreated AD serum, or V8 treated AD serum) were included for further processing. Peptide intensity values were transformed (log2), and missing values imputed using Perseus' default parameters. Aminobiotinylation produced only four matrices, one for each condition, while TAILS produced eight, due to the separate heavy and light dimethylation MaxQuant searches, and for N-terminal acetylation and pyroglutamation. For TAILS analysis, matrices were further processed by summing the intensities of matched peptides between N-terminal dimethylation and N-terminal acetylation/pyroglutamation, in both the heavy and light searches. See QUANTIFICATION AND STATISTICAL ANALYSIS for further details. Pre-TAILS analysis, i.e., peptides that underwent mass spectrometry without enrichment with HPG-ALD polymer to quantify proteins/peptides in the untreated and V8 treated conditions was also performed using the same parameters as above, but with N-terminal dimethylation set as a variable modification.

SDS-PAGE and Immunoblotting—SDS-PAGE was performed using 12 % self-cast gels (Mini-PROTEAN® Tetra handcast system, BioRad), or 4–20 % gradient gels (BioRad), and run using a Mini-PROTEAN Tetra cell (BioRad). Gels were stained with InstantBlue (Expedeon) or used directly for immunoblotting. Proteins were transferred to PVDF membranes using a Trans-Blot SD semi-dry system (BioRad), with transfer confirmed using Ponceau stain prior to blocking with 5 % milk in Tris buffered saline–Tween 20 (this blotting buffer was used for subsequent wash steps and antibody incubations), for 1 hour at room temperature or 4°C for 16 hours. Blots were exposed to primary antibody (see below) at dilutions of 1:1000 antibody: blotting buffer for 2 hours and then washed three times for 15 minutes. Next, secondary antibody at a 1:5000 dilution (anti-rabbit IgG -HRP conjugate,

Cell Signaling Technologies) was incubated with blots for 1 hour, washed three times for 15 minutes, then exposed to the Supersignal West Pico chemiluminescent substrate (Thermo Fisher). Blots were imaged with developing film (exposure from 5 minutes-16 hours), or with an imaging system (ChemDoc XRS imager, BioRad). Proteins analyzed by immunoblotting, and their corresponding primary antibodies, were: Prothrombin/thrombin (rabbit monoclonal, Abcam, cat. no. ab208589), SERPINC1/antithrombin-III (rabbit polyclonal, ThermoFisher, cat. no. PA513674), α2-macroglobulin (rabbit polyclonal, ThermoFisher, cat. no. PA529584), SERPINA1/α1-antitrypsin (rabbit polyclonal, ThermoFisher, cat. no. 711079), complement C3 (rabbit monoclonal, Abcam, cat. no. ab200999), complement C4b-rabbit polyclonal (ThermoFisher, cat. no. PA529147), and transferrin (rabbit polyclonal, ThermoFisher, cat. no. PA3913). Linear schematics of proteins assessed by western blot were rendered using illustrator for biological sequences (IBS, http://ibs.biocuckoo.org/; Liu et al.,2015) and labeled with cleavage sites identified by N-terminomics.

Induction of protease expression, zymography, and serum digest by culture supernatants—Strains containing pAFLS1 (EV), -*aur*, or -*sspA* were routinely passaged as described, picked from agar plates, and incubated for 16 hours in TSB with 10 μg/ml Chl, 0.8 μM $CdCl_2$. Cells were removed by centrifugation at 3000 g for 10 minutes, and culture supernatants concentrated using a 3 kDa Mw cutoff centrifugal filter (Millipore-Sigma) and centrifugation at 3000 g for 1 hour. This typically resulted in 20-fold concentration, as measured by volume reduction (2 mL to 100 μl). Concentrated supernatants underwent zymography as previously described (Shaw et al., 2004), with protein concentration in each culture supernatant obtained by 660 nm assay (ThermoFisher Scientific) and standardized to the lowest concentration in any given experiment. During experiments to test Aur inhibition, zymogram developing buffers were either used as described or modified to exclude 5 mM $CaCl_2$, and include 100 mM sodium citrate or 20 mM 1,10-phenanthroline to sequester metals. Concentrated culture supernatants were also used in serum digest experiments. In these cases, variable concentrations of serum and bacterial supernatants (indicated in the relevant results sections and in figure legends) were incubated together, in the presence or absence of 20 mM 1,10-phenanthroline, at 37°C for 16 hours. These then underwent Immunoblotting as described above.

Serum survival assay—Strains (LAC EV, Δ*sspA* EV, and Δ*sspA* +*sspA*) were routinely passaged as described, picked from agar plates, and incubated for 16 hours in TSB with 10 μg/ml Chl. These were then synchronized to early log growth phase for 3 hr at 37°C, in TSB with 10 μg/ml Chl and 0.8 μM $CdCl_2$. Cells were standardized by obtaining the volume of culture required for an OD_{600} of 0.05 in 1 ml, followed by washing twice via centrifugation (2 mins at 5000 g) and resuspension in PBS. Standardized cultures were pelleted again, and resuspended to an OD_{600} of 0.05 in 1 mL human serum with 10 μg/ml Chl and 0.8 μM $CdCl_2$. The infected human serum was incubated at 37°C with rotation. Viable bacteria were obtained over time (at 0, 2, 3, 4, 5, and 24 h), by serial dilutions and plating onto TSA.

QUANTIFICATION AND STATISTICAL ANALYSIS

Assigning significance to V8-generated Neo-N-termini—After processing in Perseus (described above in Data Processing), log2 intensities of TAILS and aminobiotinylated peptides were used in unpaired two tailed t tests (using the Microsoft Excel function “TTEST”). At this point, reverse peptides, and peptides identified as originating from non-human serum proteins, i.e., contaminants (a total of 8 peptides originating from porcine trypsin, bovine serum albumin, and *S. aureus* V8) were excluded across all conditions. Table S1 lists the mean peptide intensity in all conditions, derived from the (Perseus-imputed) peptide intensity from three experiments, where each experiment was injected into the mass spectrometer twice, resulting in n = 6 (peptides had been excluded if present in < 2 experiments). Rather than asterisks, the P value is reported. Unsurprisingly, all peptides that were unique to V8-treated conditions were statistically significant (where p = < 0.05). Those peptides unique to V8-treated conditions were used to generate Figures 2, 3, and part of Figure 4. This method of N-terminome analysis differs from previously described analyses due to its emphasis on unique N-terminal peptides, but highlights putative cleavage sites for the exogenous protease (V8 in this study), and is thus useful for studies of pathogen proteases in the host. Pre-TAILS statistical analysis, i.e., peptides that underwent mass spectrometry without enrichment with HPG-ALD polymer to quantify proteins/ peptides in the untreated and V8 treated conditions, was also performed. This was processed in the same fashion as for the enriched peptides as above. Table S2 lists the mean peptide intensity in all conditions, derived from the (Perseus-imputed) peptide intensity from three experiments, where each experiment was injected into the mass spectrometer twice, resulting in n = 6. However, no statistical analysis was performed, peptides were only assigned as unique (or not) to V8 conditions, and pre- and post- TAILS enriched conditions. This enabled a binary comparison (i.e., Is a peptide unique or not unique to a given condition?) during assessment of TAILS’ efficacy in N-terminome enrichment. Table S2 was used to generate supplemental Figure S1. For serum survival assays, the statistical methods are explained in the legend of Figure 6.

Supplementary Material

Refer to Web version on PubMed Central for supplementary material.

ACKNOWLEDGMENTS

All authors are employed by the University of South Florida. A.M.F. is partly funded by the Fulbright-Genschaft USF Postdoctoral scholarship award and is a member of the American Society for Microbiology (ASM) and the Human Proteome Organisation (HUPO). L.N.S. is a fellow of the American Association for the Advancement of Science (AAAS) and member of the ASM. This work was supported by AI124458 (L.N.S.) from the National Institute of Allergy and Infectious Diseases. The authors would like to acknowledge the key role of the University of South Florida’s Cell, Microbiology, and Molecular Biology department core proteomics facility.

REFERENCES

Almitairi JOM, Venkatraman Girija U, Furze CM, Simpson-Gray X, Badakshi F, Marshall JE, Schwaeble WJ, Mitchell DA, Moody PCE, and Wallis R (2018). Structure of the C1r-C1s interaction of the C1 complex of complement activation. Proc. Natl. Acad. Sci. USA 115, 768–773. [PubMed: 29311313]

auf dem Keller U, Prudova A, Eckhard U, Fingleton B, and Overall CM (2013). Systems-level analysis of proteolytic events in increased vascular permeability and complement activation in skin inflammation. Sci. Signal 6, rs2. [PubMed: 23322905]

Beaufort N, Wojciechowski P, Sommerhoff CP, Szmyd G, Dubin G, Eick S, Kellermann J, Schmitt M, Potempa J, and Magdolen V (2008). The human fibrinolytic system is a target for the staphylococcal metalloprotease aureolysin. Biochem. J 410, 157–165. [PubMed: 17973626]

Berry IJ, Jarocki VM, Tacchi JL, Raymond BBA, Widjaja M, Padula MP, and Djordjevic SP (2017). N-terminomics identifies widespread endoproteolysis and novel methionine excision in a genome-reduced bacterial pathogen. Sci. Rep 7, 11063. [PubMed: 28894154]

Bhagwat SR, Hajela K, Bhutada S, Choudhary K, Saxena M, Sharma S, and Kumar A (2020). Identification of unexplored substrates of the serine protease, thrombin, using N-terminomics strategy. Int. J. Biol. Macromol 144, 449–459. [PubMed: 31862363]

Boles BR, and Horswill AR (2008). Agr-mediated dispersal of Staphylococcus aureus biofilms. PLoS Pathog 4, e1000052. [PubMed: 18437240]

Bowen ME, and Gettins PGW (1998). Bait region involvement in the dimerdimer interface of human α 2-macroglobulin and in mediating gross conformational change. Evidence from cysteine variants that form interdimer disulfides.J. Biol. Chem 273, 1825–1831. [PubMed: 9430734]

Brömme D, Peters K, Fink S, and Fittkau S (1986). Enzyme-substrate interactions in the hydrolysis of peptide substrates by thermitase, subtilisin BPN', and proteinase K. Arch. Biochem. Biophys 244, 439–446. [PubMed: 3511847]

Byrum SD, Loughran AJ, Beenken KE, Orr LM, Storey AJ, Mackintosh SG, Edmondson RD, Tackett AJ, and Smeltzer MS (2018). Label-Free Proteomic Approach to Characterize Protease-Dependent and -Independent Effects of sarA Inactivation on the Staphylococcus aureus Exoproteome. J. Proteome Res 17, 3384–3395. [PubMed: 30209945]

Calander AM, Jonsson IM, Kanth A, Arvidsson S, Shaw L, Foster SJ, and Tarkowski A (2004). Impact of staphylococcal protease expression on the outcome of infectious arthritis. Microbes Infect. 6, 202–206. [PubMed: 14998519]

Chromy BA, Gonzales AD, Perkins J, Choi MW, Corzett MH, Chang BC, Corzett CH, and McCutchen-Maloney SL (2004). Proteomic analysis of human serum by two-dimensional differential gel electrophoresis after depletion of high-abundant proteins. J. Proteome Res 3, 1120–1127. [PubMed: 15595720]

Coffey MJ, Dagley LF, Seizova S, Kapp EA, Infusini G, Roos DS, Boddey JA, Webb AI, and Tonkin CJ (2018). Aspartyl Protease 5 Matures Dense Granule Proteins That Reside at the Host-Parasite Interface in Toxoplasma gondii. MBio 9, 1–21.

Colaert N, Helsens K, Martens L, Vandekerckhove J, and Gevaert K (2009). Improved visualization of protein consensus sequences by iceLogo. Nat. Methods 6, 786–787. [PubMed: 19876014]

Coulter SN, Schwan WR, Ng EY, Langhorne MH, Ritchie HD, Westbrock-Wadman S, Hufnagle WO, Folger KR, Bayer AS, and Stover CK (1998). Staphylococcus aureus genetic loci impacting growth and survival in multiple infection environments. Mol. Microbiol 30, 393–404. [PubMed: 9791183]

Cox J, and Mann M (2008). MaxQuant enables high peptide identification rates, individualized p.p.b.-range mass accuracies and proteome-wide protein quantification. Nat. Biotechnol 26, 1367–1372. [PubMed: 19029910]

Drapeau GR (1978). Role of metalloprotease in activation of the precursor of staphylococcal protease. J. Bacteriol 136, 607–613. [PubMed: 711676]

Drapeau GR, Boily Y, and Houmard J (1972). Purification and properties of an extracellular protease of Staphylococcus aureus. J. Biol. Chem 247, 6720–6726. [PubMed: 4627743]

Ellington JK, Elhofy A, Bost KL, and Hudson MC (2001). Involvement of mitogen-activated protein kinase pathways in Staphylococcus aureus invasion of normal osteoblasts. Infect. Immun 69, 5235–5242. [PubMed: 11500391]

Elmwall J, Kwiecinski J, Na M, Ali AA, Osla V, Shaw LN, Wang W, Sävman K, Josefsson E, Bylund J, et al. (2017). Galectin-3 is a target for proteases involved in the virulence of Staphylococcus aureus. Infect. Immun 85, 6–8.

Fey PD, Endres JL, Yajjala VK, Widhelm TJ, Boissy RJ, Bose JL, and Bayles KW (2013). A genetic resource for rapid and comprehensive phenotype screening of nonessential Staphylococcus aureus genes. MBio 4, e00537, e12. [PubMed: 23404398]

Haudenschild DR, Eldridge A, Lein PJ, and Chromy BA (2014). High abundant protein removal from rodent blood for biomarker discovery. Biochem. Biophys. Res. Commun 455, 84–89. [PubMed: 25445603]

Hill ME, Kumar A, Wells JA, Hobman TC, Julien O, and Hardy JA (2018). The Unique Cofactor Region of Zika Virus NS2B-NS3 Protease Facilitates Cleavage of Key Host Proteins. ACS Chem. Biol 13, 2398–2405. [PubMed: 30080377]

Imamura T, Tanase S, Szmyd G, Kozik A, Travis J, and Potempa J (2005). Induction of vascular leakage through release of bradykinin and a novel kinin by cysteine proteinases from Staphylococcus aureus. J. Exp. Med 201, 1669–1676. [PubMed: 15897280]

Impens F, Rolhion N, Radoshevich L, Bécavin C, Duval M, Mellin J, García Del Portillo F, Pucciarelli MG, Williams AH, and Cossart P (2017). N-terminomics identifies Prli42 as a membrane miniprotein conserved in Firmicutes and critical for stressosome activation in Listeria monocytogenes. Nat. Microbiol 2, 17005. [PubMed: 28191904]

Jagdeo JM, Dufour A, Klein T, Solis N, Kleifeld O, Kizhakkedathu J, Luo H, Overall CM, and Jan E (2018). N-Terminomics TAILS Identifies Host Cell Substrates of Poliovirus and Coxsackievirus B3 3C Proteinases That Modulate Virus Infection. J. Virol 92, 1–23.

Jusko M, Potempa J, Kantyka T, Bielecka E, Miller HK, Kalinska M, Dubin G, Garred P, Shaw LN, and Blom AM (2014). Staphylococcal proteases aid in evasion of the human complement system. J. Innate Immun 6, 31–46. [PubMed: 23838186]

Kantyka T, Plaza K, Koziel J, Florczyk D, Stennicke HR, Thogersen IB, Enghild JJ, Silverman GA, Pak SC, and Potempa J (2011). Inhibition of Staphylococcus aureus cysteine proteases by human serpin potentially limits staphylococcal virulence. Biol. Chem 392, 483–489. [PubMed: 21476872]

Kleifeld O, Doucet A, auf dem Keller U, Prudova A, Schilling O, Kainthan RK, Starr AE, Foster LJ, Kizhakkedathu JN, and Overall CM (2010). Isotopic labeling of terminal amines in complex samples identifies protein N-termini and protease cleavage products. Nat. Biotechnol 28, 281–288. [PubMed: 20208520]

Kleifeld O, Doucet A, Prudova A, auf dem Keller U, Gioia M, Kizhakkedathu JN, and Overall CM (2011). Identifying and quantifying proteolytic events and the natural N terminome by terminal amine isotopic labeling of substrates. Nat. Protoc 6, 1578–1611. [PubMed: 21959240]

Kolar SL, Ibarra JA, Rivera FE, Mootz JM, Davenport JE, Stevens SM, Horswill AR, and Shaw LN (2013). Extracellular proteases are key mediators of Staphylococcus aureus virulence via the global modulation of virulence-determinant stability. MicrobiologyOpen 2, 18–34. [PubMed: 23233325]

Kreiswirth BN, Löfdahl S, Betley MJ, O'Reilly M, Schlievert PM, Bergdoll MS, and Novick RP (1983). The toxic shock syndrome exotoxin structural gene is not detectably transmitted by a prophage. Nature 305, 709–712. [PubMed: 6226876]

Laarman AJ, Ruyken M, Malone CL, van Strijp JA, Horswill AR, and Rooijakkers SH (2011). Staphylococcus aureus metalloprotease aureolysin cleaves complement C3 to mediate immune evasion. J. Immunol 186, 6445–6453. [PubMed: 21502375]

Laarman AJ, Mijnheer G, Mootz JM, van Rooijen WJ, Ruyken M, Malone CL, Heezius EC, Ward R, Milligan G, van Strijp JA, et al. (2012). Staphylococcus aureus Staphopain A inhibits CXCR2-dependent neutrophil activation and chemotaxis. EMBO J 31, 3607–3619. [PubMed: 22850671]

Lan J, Núñez Galindo A, Doecke J, Fowler C, Martins RN, Rainey-Smith SR, Cominetti O, and Dayon L (2018). Systematic Evaluation of the Use of Human Plasma and Serum for Mass-Spectrometry-Based Shotgun Proteomics. J. Proteome Res 17, 1426–1435. [PubMed: 29451788]

Lange PF, Huesgen PF, Nguyen K, and Overall CM (2014). Annotating N termini for the human proteome project: N termini and Nα-acetylation status differentiate stable cleaved protein species from degradation remnants in the human erythrocyte proteome. J. Proteome Res 13, 2028–2044. [PubMed: 24555563]

Liu Z, Zhou X, Shapiro SD, Shipley JM, Twining SS, Diaz LA, Senior RM, and Werb Z (2000). The serpin α1-proteinase inhibitor is a critical substrate for gelatinase B/MMP-9 in vivo. Cell 102, 647–655. [PubMed: 11007483]

Liu W, Xie Y, Ma J, Luo X, Nie P, Zuo Z, Lahrmann U, Zhao Q, Zheng Y, Zhao Y, et al. (2015). IBS: an illustrator for the presentation and visualization of biological sequences. Bioinformatics 31, 3359–3361. [PubMed: 26069263]

Loeb L (1903). The influence of certain bacteria on the coagulation of the blood. J. Med. Res 10, 407–419. [PubMed: 19971581]

Losse J, Zipfel PF, and Józsi M (2010). Factor H and factor H-related protein 1 bind to human neutrophils via complement receptor 3, mediate attachment to Candida albicans, and enhance neutrophil antimicrobial activity.J. Immunol 184, 912–921. [PubMed: 20008295]

Loughran AJ, Atwood DN, Anthony AC, Harik NS, Spencer HJ, Beenken KE, and Smeltzer MS (2014). Impact of individual extracellular proteases on Staphylococcus aureus biofilm formation in diverse clinical isolates and their isogenic sarA mutants. MicrobiologyOpen 3, 897–909. [PubMed: 25257373]

Marino G, Eckhard U, and Overall CM (2015). Protein Termini and Their Modifications Revealed by Positional Proteomics. ACS Chem. Biol 10, 1754–1764. [PubMed: 26042555]

Markert Y, Köditz J, Ulbrich-Hofmann R, and Arnold U (2003). Proline versus charge concept for protein stabilization against proteolytic attack. Protein Eng. 16, 1041–1046. [PubMed: 14983085]

Marshall NC, Finlay BB, and Overall CM (2017). Sharpening Host Defenses during Infection: Proteases Cut to the Chase. Mol. Cell. Proteomics 16 (4, suppl 1), S161–S171. [PubMed: 28179412]

McAdow M, Missiakas DM, and Schneewind O (2012). Staphylococcus aureus secretes coagulase and von Willebrand factor binding protein to modify the coagulation cascade and establish host infections. J. Innate Immun 4, 141–148. [PubMed: 22222316]

Moks T, Abrahmsén L, Nilsson B, Hellman U, Sjöquist J, and Uhlén M (1986). Staphylococcal protein A consists of five IgG-binding domains. Eur. J. Biochem 156, 637–643. [PubMed: 2938951]

Molla A, Yamamoto T, Akaike T, Miyoshi S, and Maeda H (1989). Activation of hageman factor and prekallikrein and generation of kinin by various microbial proteinases. J. Biol. Chem 264, 10589–10594. [PubMed: 2499581]

Nickerson NN, Prasad L, Jacob L, Delbaere LT, and McGavin MJ (2007). Activation of the SspA serine protease zymogen of Staphylococcus aureus proceeds through unique variations of a trypsinogen-like mechanism and is dependent on both autocatalytic and metalloprotease-specific processing. J. Biol. Chem 282, 34129–34138. [PubMed: 17878159]

Nickerson NN, Joag V, and McGavin MJ (2008). Rapid autocatalytic activation of the M4 metalloprotease aureolysin is controlled by a conserved N-terminal fungalysin-thermolysin-propeptide domain. Mol. Microbiol 69, 1530–1543. [PubMed: 18673454]

Nickerson N, Ip J, Passos DT, and McGavin MJ (2010). Comparison of Staphopain A (ScpA) and B (SspB) precursor activation mechanisms reveals unique secretion kinetics of proSspB (Staphopain B), and a different interaction with its cognate Staphostatin, SspC. Mol. Microbiol 75, 161–177. [PubMed: 19943908]

Norton R, Heuzenroeder M, and Manning PA (1996). Non-specific serum binding to streptavidin in a biotinylated peptide based enzyme immunoassay.J. Immunoassay 17, 195–204.

Overall CM, and Dean RA (2006). Degradomics: systems biology of the protease web. Pleiotropic roles of MMPs in cancer. Cancer Metastasis Rev 25, 69–75. [PubMed: 16680573]

Pan ES, et al. (2004). Increasing prevalence of methicillin-resistant staphylococcus aureus infection in California jails. Infect. Dis. Clin. Pract 12, 210.

Perez-Riverol Y, Csordas A, Bai J, Bernal-Llinares M, Hewapathirana S, Kundu DJ, Inuganti A, Griss J, Mayer G, Eisenacher M, et al. (2019). The PRIDE database and related tools and resources in 2019: improving support for quantification data. Nucleic Acids Res 47 (D1), D442–D450. [PubMed: 30395289]

Potempa J, Watorek W, and Travis J (1986). The inactivation of human plasma α1-proteinase inhibitor by proteinases from Staphylococcus aureus.J. Biol. Chem 261, 14330–14334. [PubMed: 3533918]

Potempa J, Dubin A, Korzus G, and Travis J (1988). Degradation of elastin by a cysteine proteinase from Staphylococcus aureus. J. Biol. Chem 263, 2664–2667. [PubMed: 3422637]

Prasad L, Leduc Y, Hayakawa K, and Delbaere LT (2004). The structure of a universally employed enzyme: V8 protease from Staphylococcus aureus. Acta Crystallogr. D Biol. Crystallogr 60, 256–259. [PubMed: 14747701]

Prokesová L, Potuzníková B, Potempa J, Zikán J, Radl J, Hachová L, Baran K, Porwit-Bobr Z, and John C (1992). Cleavage of human immunoglobulins by serine proteinase from Staphylococcus aureus. Immunol. Lett 31, 259–265. [PubMed: 1372285]

Prudova A, Gocheva V, Auf dem Keller U, Eckhard U, Olson OC, Akkari L, Butler GS, Fortelny N, Lange PF, Mark JC, et al. (2016). TAILS N-Terminomics and Proteomics Show Protein Degradation Dominates over Proteolytic Processing by Cathepsins in Pancreatic Tumors. Cell Rep. 16, 1762–1773. [PubMed: 27477282]

Pustelny K, Zdzalik M, Stach N, Stec-Niemczyk J, Cichon P, Czarna A, Popowicz G, Mak P, Drag M, Salvesen GS, et al. (2014). Staphylococcal SplB serine protease utilizes a novel molecular mechanism of activation.J. Biol. Chem 289, 15544–15553. [PubMed: 24713703]

Ramirez AM, Beenken KE, Byrum SD, Tackett AJ, Shaw LN, Gimza BD, and Smeltzer MS (2020). SarA plays a predominant role in controlling the production of extracellular proteases in the diverse clinical isolates of Staphylococcus aureus LAC and UAMS-1. Virulence 11, 1738–1762. [PubMed: 33258416]

Rapala-Kozik M, Potempa J, Nelson D, Kozik A, and Travis J (1999). Comparative cleavage sites within the reactive-site loop of native and oxidized α1-proteinase inhibitor by selected bacterial proteinases. Biol. Chem 380, 1211–1216. [PubMed: 10595584]

Rawlings ND, Barrett AJ, Thomas PD, Huang X, Bateman A, and Finn RD (2018). The MEROPS database of proteolytic enzymes, their substrates and inhibitors in 2017 and a comparison with peptidases in the PANTHER database. Nucleic Acids Res. 46, D624–D632. [PubMed: 29145643]

Reed SB, Wesson CA, Liou LE, Trumble WR, Schlievert PM, Bohach GA, and Bayles KW (2001). Molecular characterization of a novel Staphylococcus aureus serine protease operon. Infect. Immun 69, 1521–1527. [PubMed: 11179322]

Rice K, Peralta R, Bast D, de Azavedo J, and McGavin MJ (2001). Description of staphylococcus serine protease (ssp) operon in Staphylococcus aureus and nonpolar inactivation of sspA-encoded serine protease. Infect. Immun 69, 159–169. [PubMed: 11119502]

Roux PP, and Blenis J (2004). ERK and p38 MAPK-activated protein kinases: a family of protein kinases with diverse biological functions. Microbiol. Mol. Biol. Rev 68, 320–344. [PubMed: 15187187]

Sabino F, Hermes O, Egli FE, Kockmann T, Schlage P, Croizat P, Kizhakkedathu JN, Smola H, and auf dem Keller U (2015). *In vivo* assessment of protease dynamics in cutaneous wound healing by degradomics analysis of porcine wound exudates. Mol. Cell. Proteomics 14, 354–370. [PubMed: 25516628]

Salier JP, Rouet P, Raguenez G, and Daveau M (1996). The inter-alphainhibitor family: from structure to regulation. Biochem. J 315, 1–9. [PubMed: 8670091]

Salisbury V, Hedges RW, and Datta N (1972). Two modes of “curing” transmissible bacterial plasmids. J. Gen. Microbiol 70, 443–452. [PubMed: 4556250]

Shaw L, Golonka E, Potempa J, and Foster SJ (2004). The role and regulation of the extracellular proteases of Staphylococcus aureus. Microbiology (Reading) 150, 217–228. [PubMed: 14702415]

Shohet JM, Pemberton P, and Carroll MC (1993). Identification of a major binding site for complement C3 on the IgG1 heavy chain. J. Biol. Chem 268, 5866–5871. [PubMed: 8449952]

Skjeflo EW, Christiansen D, Fure H, Ludviksen JK, Woodruff TM, Espevik T, Nielsen EW, Brekke OL, and Mollnes TE (2018). Staphylococcus aureus-induced complement activation promotes tissue factor-mediated coagulation. J. Thromb. Haemost 16, 905–918. [PubMed: 29437288]

Slade DJ, Lovelace LL, Chruszcz M, Minor W, Lebioda L, and Sodetz JM (2008). Crystal structure of the MACPF domain of human complement protein C8 alpha in complex with the C8 gamma subunit. J. Mol. Biol 379, 331–342. [PubMed: 18440555]

Smith EJ, Visai L, Kerrigan SW, Speziale P, and Foster TJ (2011). The Sbi protein is a multifunctional immune evasion factor of Staphylococcus aureus. Infect. Immun 79, 3801–3809. [PubMed: 21708997]

Sørensen SB, Sørensen TL, and Breddam K (1991). Fragmentation of proteins by S. aureus strain V8 protease. Ammonium bicarbonate strongly inhibits the enzyme but does not improve the selectivity for glutamic acid. FEBS Lett. 294, 195–197. [PubMed: 1684551]

Stach N, Kalinska M, Zdzalik M, Kitel R, Karim A, Serwin K, Rut W, Larsen K, Jabaiah A, Firlej M, et al. (2018). Unique Substrate Specificity of SplE Serine Protease from Staphylococcus aureus. Structure 26, 572–579.e4. [PubMed: 29526434]

Stentzel S, Teufelberger A, Nordengrün M, Kolata J, Schmidt F, van Crombruggen K, Michalik S, Kumpfmüller J, Tischer S, Schweder T, et al. (2017). Staphylococcal serine protease-like proteins are pacemakers of allergic airway reactions to Staphylococcus aureus. J. Allergy Clin. Immunol 139, 492–500. [PubMed: 27315768]

Sullivan MA, Yasbin RE, and Young FE (1984). New shuttle vectors for Bacillus subtilis and Escherichia coli which allow rapid detection of inserted fragments. Gene 29, 21–26. [PubMed: 6092222]

Suzuki K, Nishioka J, and Hayashi T (1990). Localization of thrombomodulin-binding site within human thrombin. J. Biol. Chem 265, 13263–13267. [PubMed: 2165498]

Timmer JC, and Salvesen GS (2011). N-terminomics: A High-Content Screen for Protease Substrates and Their Cleavage Sites. Methods Mol Biol. 753, 243–255. [PubMed: 21604127]

Wegrzynowicz Z, Heczko PB, Drapeau GR, Jeljaszewicz J, and Pulverer G (1980). Prothrombin activation by a metalloprotease from Staphylococcus aureus. J. Clin. Microbiol 12, 138–139. [PubMed: 6785302]

Weidmann H, Heikaus L, Long AT, Naudin C, Schlüter H, and Reneé T (2017). The plasma contact system, a protease cascade at the nexus of inflammation, coagulation and immunity. Biochim. Biophys. Acta Mol. Cell Res 1864, 2118–2127. [PubMed: 28743596]

Windham IH, Chaudhari SS, Bose JL, Thomas VC, and Bayles KW (2016). SrrAB modulates Staphylococcus aureus cell death through regulation of cidABC transcription. J. Bacteriol 198, 1114–1122. [PubMed: 26811317]

Yang L, Li Y, Bhattacharya A, and Zhang Y (2016). A plasma proteolysis pathway comprising blood coagulation proteases. Oncotarget 7, 40919–40938. [PubMed: 27248165]

Zdzalik M, Kalinska M, Wysocka M, Stec-Niemczyk J, Cichon P, Stach N, Gruba N, Stennicke HR, Jabaiah A, Markiewicz M, et al. (2013). Biochemical and structural characterization of SplD protease from Staphylococcus aureus. PLoS ONE 8, e76812. [PubMed: 24130791]

Zheng J, et al. (2014). A secreted bacterial protease tailors the Staphylococcus aureus virulence repertoire to modulate bone remodeling during osteomyelitis. Cell Host Microbe 60, 186–196.

Highlights

- N-terminomics can be used to identify bacterial protease targets in complex human samples
- *S. aureus* V8 protease cleaves human serum proteins with probable consequences for disease
- V8 heavily impacts clotting, complement, and protease inhibitor networks

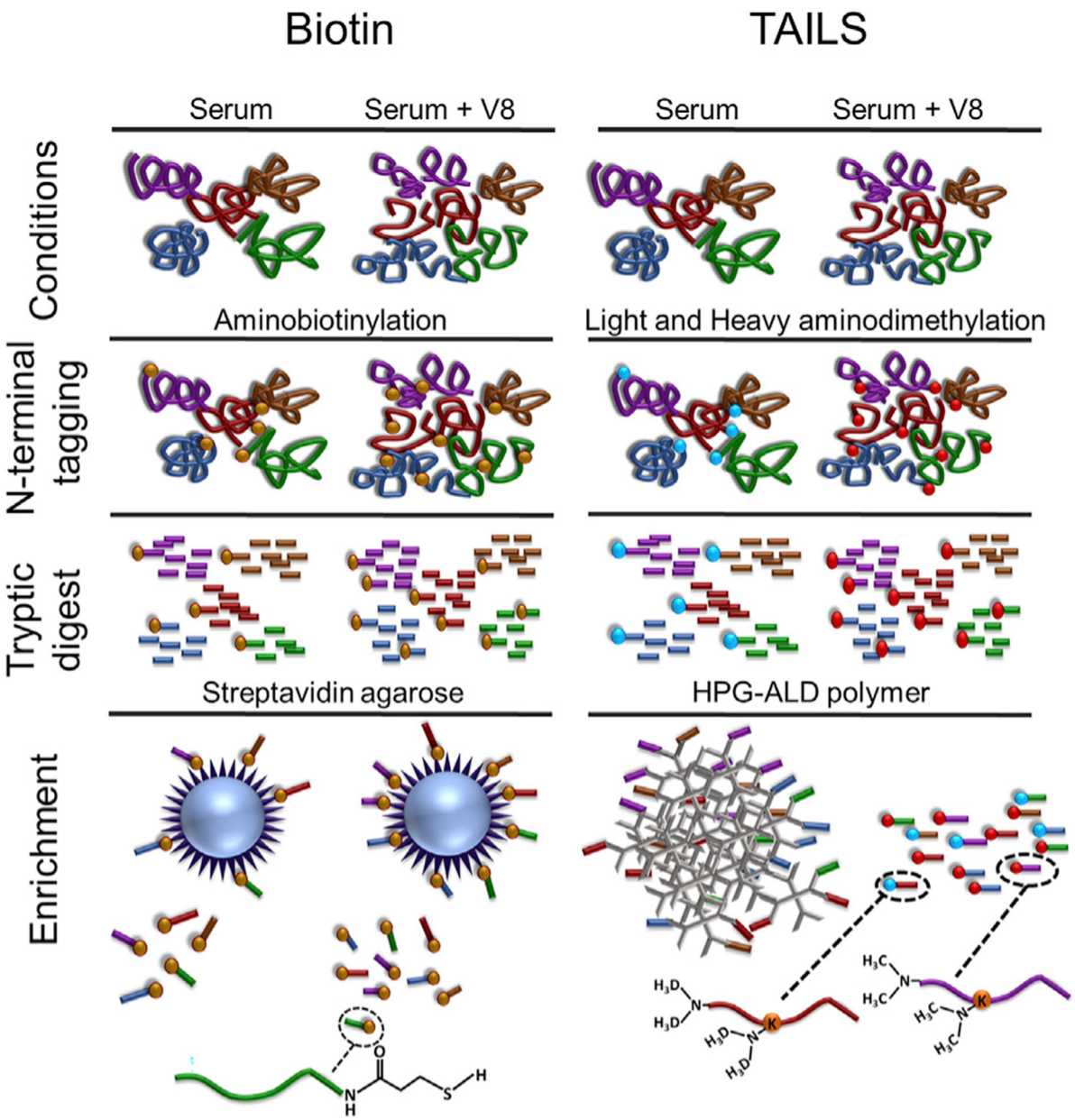

Figure 1. Comparison of aminobiotinylation (biotin) and TAILS methodologies

Serum or AD serum, +/− V8 protease. Proteolysis produces neo-N termini, in addition to native N termini. Amino tagging is performed at this stage. In aminobiotinylation, lysines were reduced to homoarginines, and terminal amines tagged with a sulfobiotin compound. For TAILS, dimethylation was used to label amines (N termini and Lys), with light and heavy reagents used for untreated and V8-treated conditions, respectively. Trypsin digestion was performed for both TAILS and aminobiotinylation. N termini from conditions that underwent aminobiotinylation were enriched with streptavidin beads and released by reducing a disulfide bond present in the sulfobiotin tag. TAILS conditions were pooled post-tryptic digest due to the different dimethyl labels for the two conditions and incubated with

HPG-ALD polymer, which binds free amines resulting from trypsin digestion. N-terminal dimethyl-labeled peptides remained in solution.

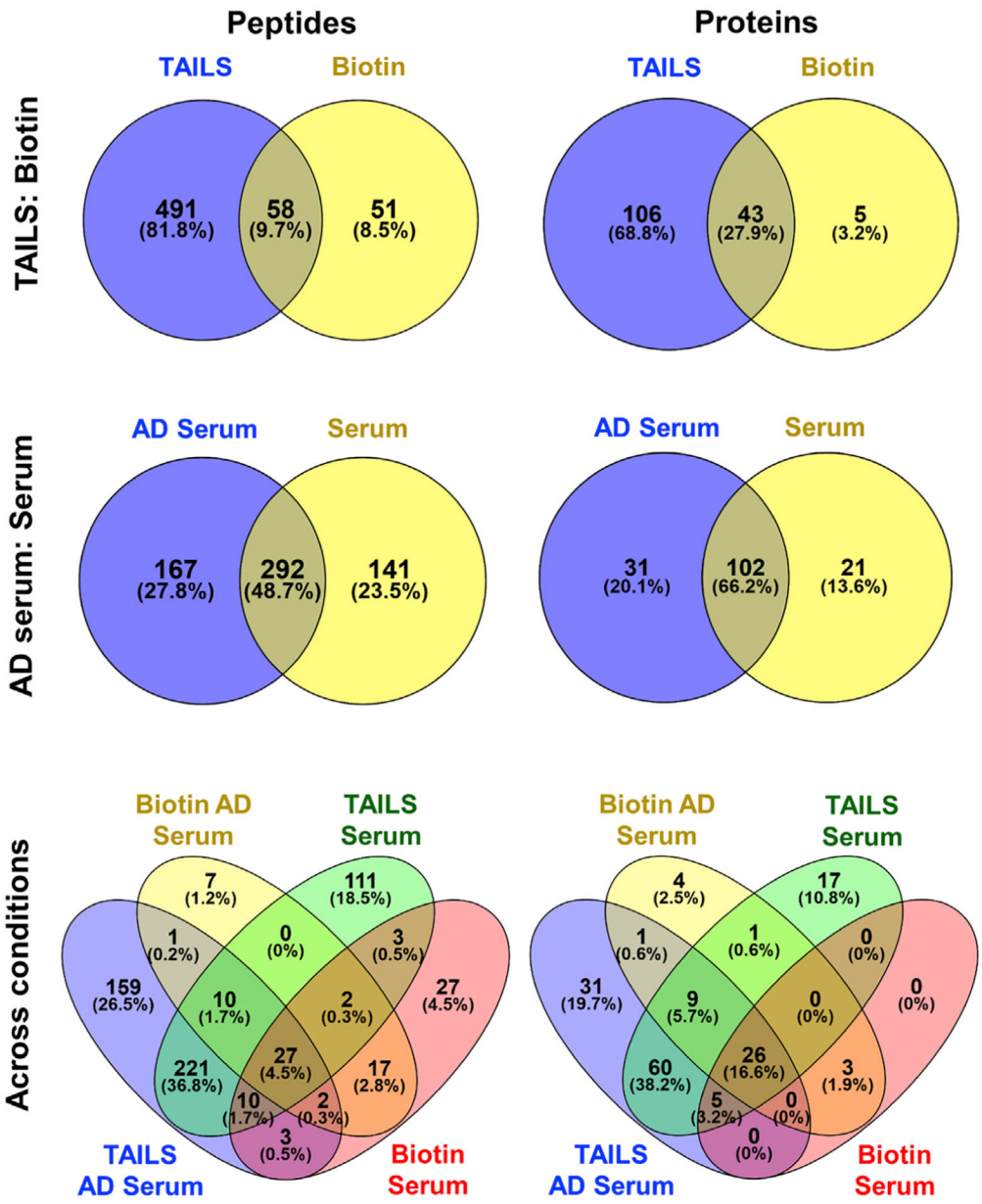

Figure 2. The impact of albumin depletion and N-terminomic method on the human serum N-terminome

Peptides and their proteins were compared between serum versus AD serum, and biotin versus TAILS. Diagrams were prepared using Venny 2.1 (https://bioinfogp.cnb.csic.es/tools/venny/index. html). See also Table S1.

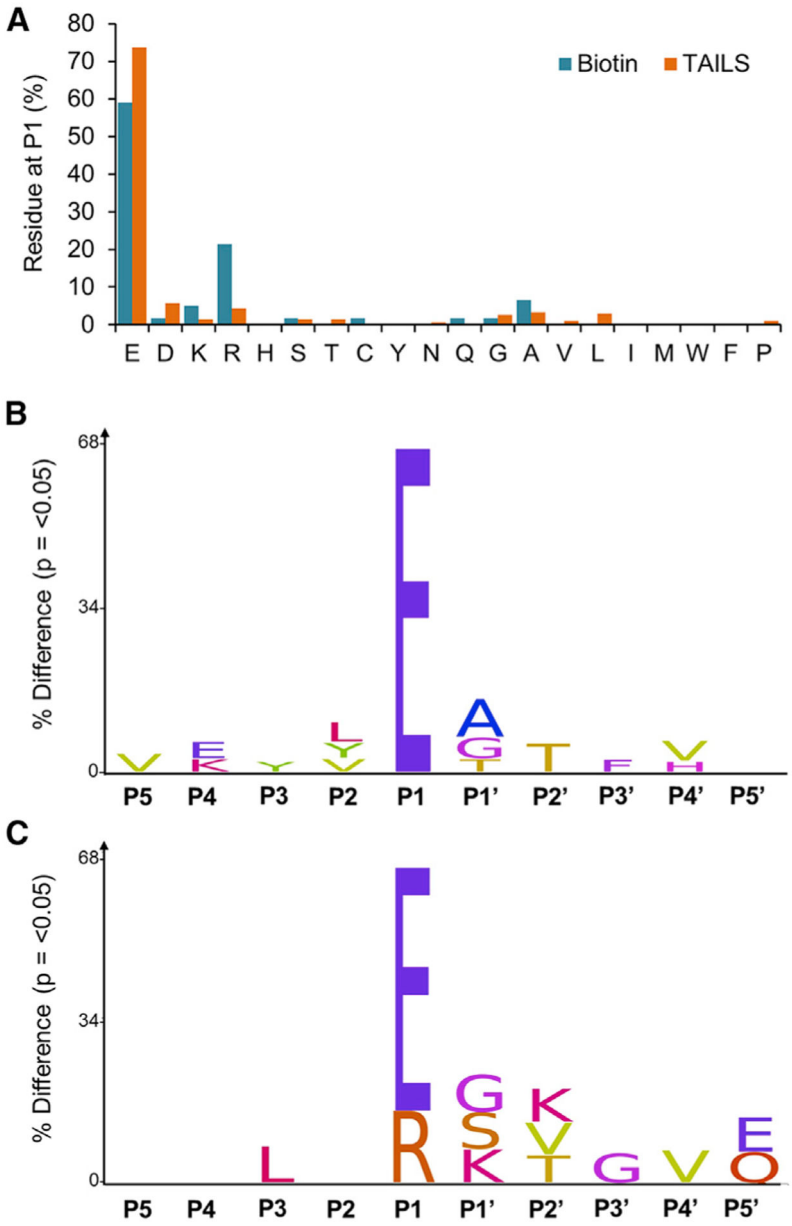

Figure 3. V8 cleavage specificity identified by N-terminomics

Percentage of each residue at P1 in Neo-N termini identified by biotin and TAILS methods of N-terminomics (blue = biotin, orange = TAILS) (A). IceLogo plots showing the percentage difference of significantly increased residues (relative to their frequency in the human proteome) in the five positions surrounding the scissile bond (P1-P1′), identified by TAILS (B) or aminobiotinylation (C). See also Figure S1.

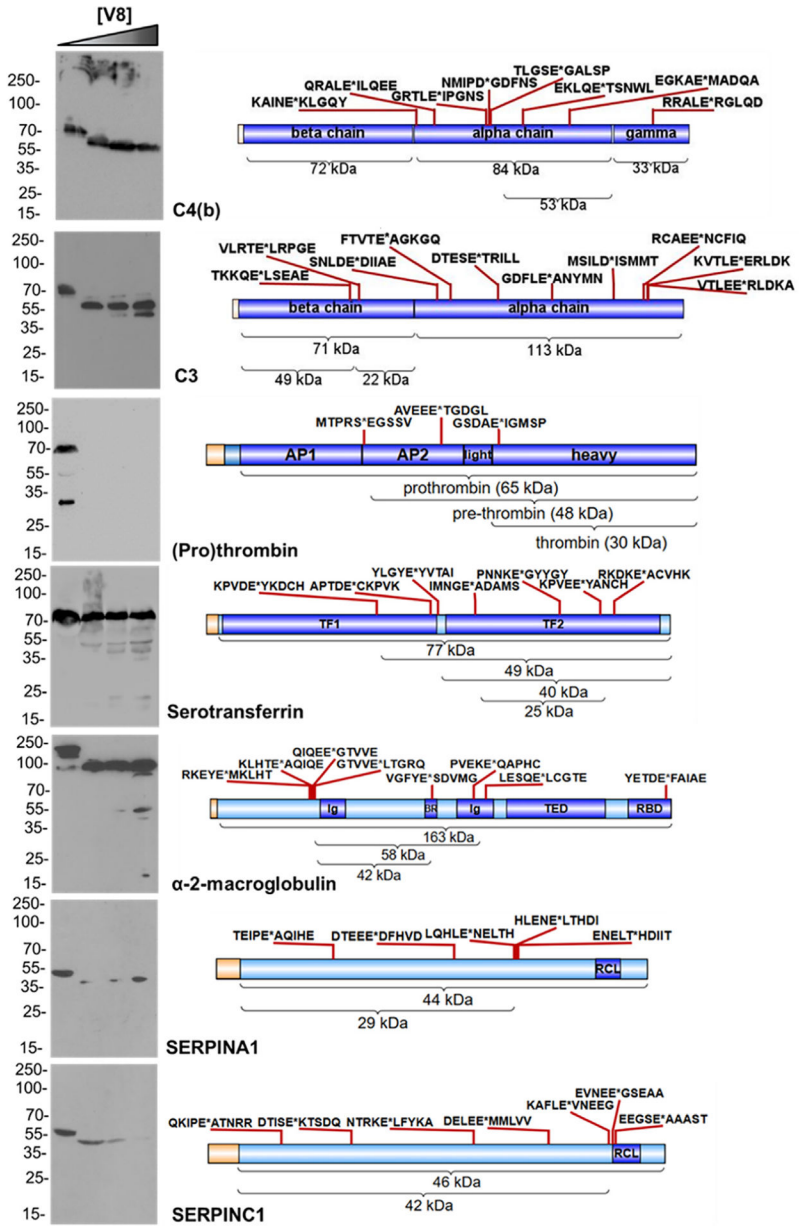

Figure 4. Validation of V8 serum substrates identified by N-terminomics

Serum was treated with varying concentrations of V8. Linear schematics depict the primary structure of proteins, with domains from UniProt/UniRef indicated. Cleavage sites inferred by N-terminomics are indicated by red markers, the scissile bond/V8 cleavage site is indicated by an asterisk with surrounding residues shown. Fragments and their ~predicted mass (calculated using ProtParam), with degradation products visible in corresponding western blots, are shown on schematics for serotransferrin, α−2-macroglobulin, SERPINA1, and SERPINC1. Prothrombin produced no visible degradation products; instead, the intact form and native products (produced by proteolytic activation) are depicted and visible in the untreated serum blot. AP1, activation peptide fragment 1; AP2, activation peptide fragment 2; light, thrombin light chain; heavy, thrombin heavy chain; TF1, Transferrin-like domain 1;

TF2, transferrin-like domain 2; Ig, Ig-like fold; BR, bait region; RBD, receptor binding domain; RCL, reactive center loop. See also Figure S4.

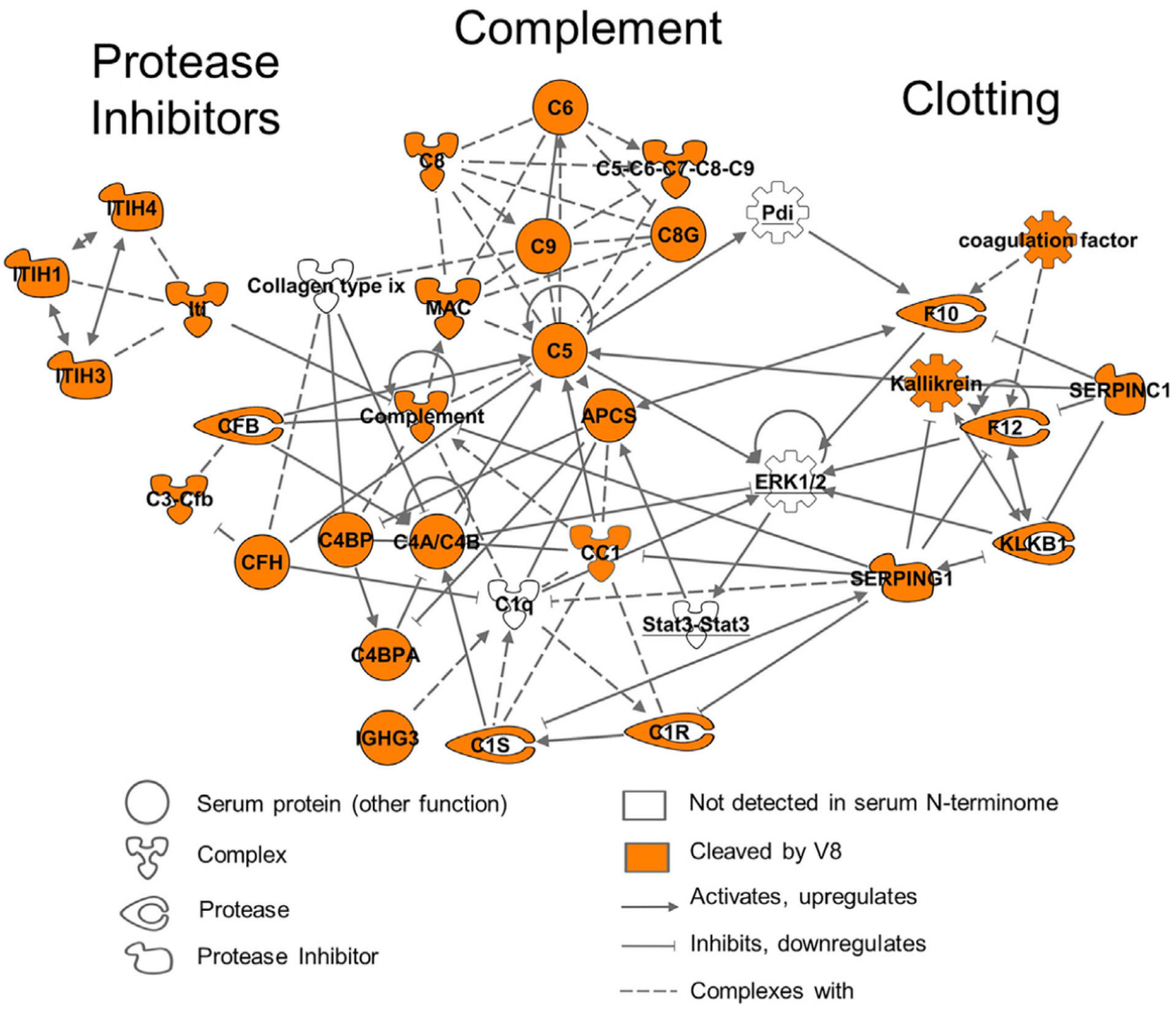

Figure 5. Network analysis of V8-cleaved proteins

Interaction analysis highlights V8 cleavage throughout an acute phase response network. Intracellular proteins are underlined and act indirectly with the indicated extracellular proteins.

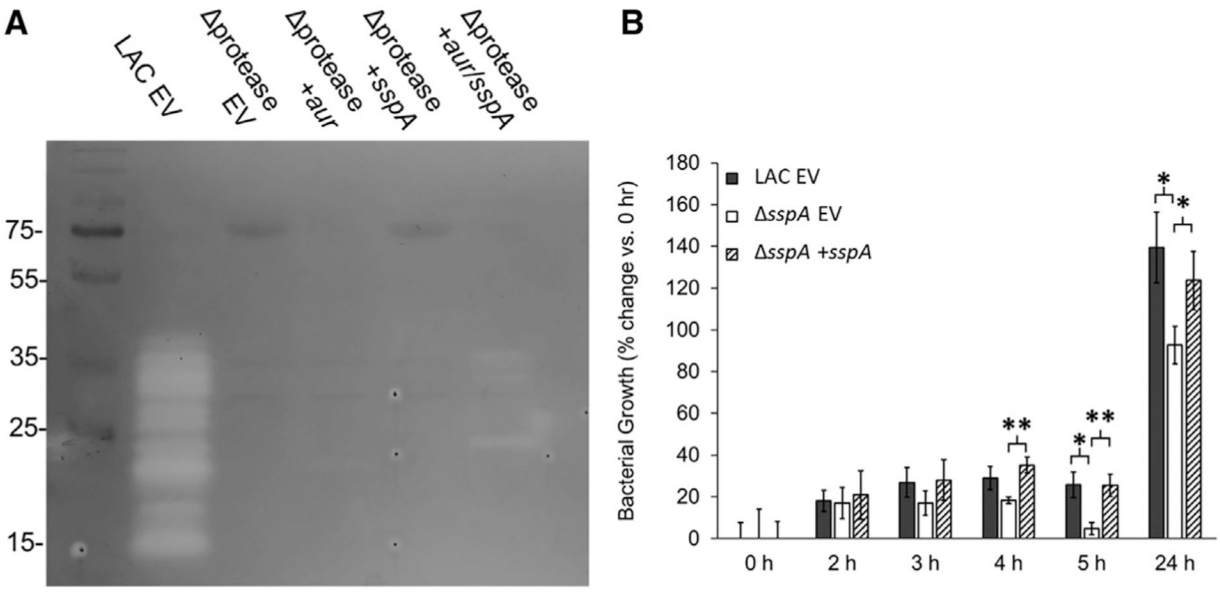

Figure 6. V8 complementation and activation by Aur and the impact of V8 expression on serum survival of *S. aureus*

(A) Gelatin zymography of concentrated culture supernatants. +*aur*/*sspA* refers to the co-culture of Δprotease strains complemented with either *aur* or *sspA*.

(B) *S. aureus* survival in 100% human serum. Cfu/mL was determined, and bacterial growth at each time point was expressed as the mean ((n = 3) percentage change relative to 0 h for each strain. Error bars, SD, significance of relative bacterial growth was assessed by unpaired t test with unequal variance, *p = < 0.05, **p = < 0.01. Comparisons between each strain were made independently at each time point. EV, empty vector (pAFLS1) was present in denoted strains.

KEY RESOURCES TABLE

REAGENT OR RESOURCE	SOURCE	IDENTIFIER
Antibodies		
Anti-Prothrombin/Thrombin (rabbit monoclonal)	Abcam	Cat#ab208589
Anti-SERPINCI/antithrombin-III (rabbit polyclonal)	ThermoFisher Scientific	Cat#PA513674; RRID:AB_2301635
Anti-α2-macroglobulin (rabbit polyclonal)	ThermoFisher Scientific	Cat#PA529584; RRID:AB_2547060
Anti-SERPINA1/α1-antitrypsin (rabbit polyclonal)	ThermoFisher Scientific	Cat#711079; RRID:AB_2662337
Anti-complement C3 (rabbit monoclonal)	Abcam	Cat#ab200999
Anti-complement C4b (rabbit polyclonal)	ThermoFisher Scientific	Cat#PA529147; RRID:AB_2546623
Anti-Transferrin (rabbit polyclonal)	ThermoFisher Scientific	Cat#PA3913; RRID:AB_889484
Anti-rabbit IgG-HRP conjugate (Goat)	Cell Signaling Technology	Cat#7074S; RRID:AB_2099233
Bacterial and virus strains		
See Table S6	N/A	N/A
Biological samples		
Human serum (type AB, pooled)	Fisher Scientific	Cat#ICN2930949
Chemicals, peptides, and recombinant proteins		
S. aureus V8 protease	Sigma Aldrich (Now Millipore Sigma)	Cat#P2922
Restriction enzyme: BamHI	New England Biolabs	Cat#R0136
Restriction enzyme: EcoRI	New England Biolabs	Cat#R0101
Restriction enzyme: SalI	New England Biolabs	Cat#R0138
Restriction enzyme: ApaI	New England Biolabs	Cat#R0114
Restriction enzyme: XhoI	New England Biolabs	Cat#R0146
T4 DNA Ligase	Promega	Cat#M1801
Deposited data		
N-terminomics: serum and V8-treated serum dataset	ProteomeXchange	PXD014797
Oligonucleotides		
See Table S6	N/A	N/A
Recombinant DNA		
pMK4 plasmid	(Sullivan et al., 1984)	N/A
pJB67 plasmid	(Windham et al., 2016)	N/A
pAFLS1 plasmid	This study.	N/A
pAFLS1-*sspA*	This study.	N/A
pAFLS1-*aur*	This study.	N/A
Software and algorithms		
MaxQuant (and Perseus)	https://www.maxquant.org/ (Cox and Mann, 2008)	RRID:SCR_014485
Other		
HPG-ALD Polymer	(Kleifeld et al., 2010) https://ubc.flintbox.com/#technologies/888fc51c-36c0-40dc-a5c9-0f176ba68293	N/A